

Bayesian Inference of Local Projections with Roughness Penalty Priors

Masahiro Tanaka*

July 7, 2019

Abstract

A local projection is a statistical framework that accounts for the relationship between an exogenous variable and an endogenous variable, measured at different time points. Local projections are often applied in impulse response analyses and direct forecasting. While local projections are becoming increasingly popular because of their robustness to misspecification and their flexibility, they are less statistically efficient than standard methods, such as vector autoregression. In this study, we seek to improve the statistical efficiency of local projections by developing a fully Bayesian approach that can be used to estimate local projections using roughness penalty priors. By incorporating such prior-induced smoothness, we can use information contained in successive observations to enhance the statistical efficiency of an inference. We apply the proposed approach to an analysis of monetary policy in the United States, showing that the roughness penalty priors successfully estimate the impulse response functions and improve the predictive accuracy of local projections.

Keywords: local projection, roughness penalty prior, Bayesian B-spline, impulse response

JEL Code: C11, C14, C51

*Graduate School of Economics, Waseda University. Address: 1-6-1, Nishi-Waseda, Shinjuku-ku, Tokyo 169-8050 Japan, Email: gspddlmit45@toki.waseda.jp.

1 Introduction

Local projections introduced by Jordà (2005) provide a statistical framework that accounts for the relationship between an exogenous variable and an endogenous variable, measured at different time points. Typical applications of local projections include impulse response analyses and direct (non-iterative) forecasting (Stock and Watson, 2007). A local projection has several advantages over standard methods, such as vector autoregression (VAR). First, it does not impose a strong assumption on the data-generating process, making it robust to misspecification. Second, it can easily deal with asymmetric and/or state-dependent impulse responses (e.g., Riera-Crichton et al., 2015; Auerbach and Gorodnichenko, 2013; Ramey and Zubairy, 2018). On the other hand, local projections have several disadvantages. First, when using a local projection, the exogenous variable must be identified beforehand. Second, a local projection is statistically less efficient than other methods, and typically obtains a wiggly impulse response function, (e.g., Ramey, 2016). In an impulse response analysis, the shape of an estimated impulse response function is of concern. Therefore, if an estimated impulse response function is wiggly and has wide confidence/credible intervals, it is difficult to interpret the result, and one might wrongly reject or accept a hypothesis. In this study, we address the second disadvantage of local projections.

In order to improve the statistical efficiency, we develop a fully Bayesian approach that can be used to estimate local projections using roughness penalty priors as well as B-spline basis expansions.¹ The proposed priors, which are adapted from Bayesian splines (Lang and Brezger, 2004), are generated from an intrinsic Gaussian Markov random field; that is, they induce random-walk behavior on a sequence of parameters. By incorporating such prior-induced smoothness, we can use information contained in successive observations to enhance the statistical efficiency of an inference. We compare the proposed approach with the existing approaches through a series of Monte Carlo experiments. The proposed approach is applied to an analysis of monetary policy shocks in the United States to show how the roughness penalty priors successively smooth impulse responses and improve statistical efficiency in terms of predictive accuracy. Furthermore, we show that such improvements are almost entirely attributable to the roughness penalty priors and not to the B-spline expansions.

There are three strands of studies related to this work. For the first, Barnichon and Matthes (2019) approximate a moving average representation of a time series using values from Gaussian basis functions. Their approximation is simpler, but much coarser than ours. As a result, their estimated impulse responses may be excessively smoothed and vulnerable to model misspecification. For the second, to smooth an impulse response estimate, Miranda-Agrippino and Ricco (2017) penalize the estimate based on deviations from an impulse response derived from an estimated VAR. However, their approach seems not to work well in cases with asymmetric and/or state-dependent impulse responses. Furthermore, their approach uses the same dataset twice. This shortcoming can be resolved if a time series is long enough to be split into training and estimation samples, but this is not the general situation in macroeconomic studies. In contrast, our approach does not require a reference model, thus it is free from these problems.

For the third, the most relevant studies are those of Barnichon and Brownlees (2019) and El-Shagi (2019), who develop frequentist methods using roughness penalties. Although our approach can be regarded as a Bayesian counterpart to theirs, it confers four additional benefits. First, our approach is more flexible than Barnichon and Brownlees's (2019) approach: they allow a single parameter to control the smoothness of all parameter sequences, whereas we can assign different smoothing parameters to individual sequences. Second, our Bayesian approach

¹See, e.g., Geweke (2005) for a general introduction to Bayesian analysis.

can evaluate credible intervals in a consistent and straightforward manner, while the frequentist approaches cannot provide a theoretically grounded confidence interval. Third, in our approach, smoothing parameters are inferred from priors, implying that we can systematically consider uncertainty in the smoothness of an impulse response. In contrast, the frequentist approach prefixes smoothing parameters; Barnichon and Brownlees (2019) choose a smoothing parameter via cross-validation, while El-Shagi (2019) determines smoothing parameters on the basis of some information criteria. Fourth, our approach has better finite-sample performance than El-Shagi’s (2019) approach, as shown in Section 5.

The rest of the paper is organized as follows. Section 2 introduces the model, the priors and the posterior simulation. Section 3 conducts a set of Monte Carlo experiments and reports the result. Section 4 demonstrates our approach in an analysis of the macroeconomic effects of monetary policy shocks in the United States. Section 5 compares the proposed approach with the existing frequentist approaches. Section 6 concludes this paper.

2 Proposed Approach

We consider two classes of local projections: those with and those without B-spline expansions.

2.1 Local Projection without B-spline expansions

2.1.1 Model

We begin by describing a local projection (Jordà, 2005). While we consider only time series data, an extension to panel data is straightforward. A model for an individual observation is given by

$$y_{t+h} = \beta_{(h)}z_t + \alpha_{(h)} + \sum_{j=1}^{J-2} \gamma_{j,(h)}w_{j,t} + u_{(h),t+h}, \quad h \in \mathcal{H}, \quad t = 1, \dots, T,$$

where $\mathcal{H} = \{h_1, \dots, h_H\} \subseteq \mathbb{N}^H$ is a set of projection points such that $h_1 < h_2 < \dots < h_H$, y_{t+h} is an endogenous variable observed at period $t+h$, $\alpha_{(h)}$ is an intercept, z_t is an exogenous variable observed at period t , $w_{1,t}, \dots, w_{J-2,t}$ are covariates, which may include lags of the endogenous and exogenous variables, $\beta_{(h)}$ and $\gamma_{j,(h)}$ are unknown coefficients, and $u_{(h),t+h}$ is a residual. The model allows asymmetric and/or state-dependent impulse responses, as in Riera-Crichton et al. (2015), Auerbach and Gorodnichenko (2013), and Ramey and Zubairy (2018). The definition of y_{t+h} and z_t depends on whether the model is used for an impulse response analysis or forecasting. For the former task, y_{t+h} denotes a response observed h periods after shock z_t occurs at t ; for the latter, z_t is one of several predictors observed at t , and y_{t+h} is an h -period-ahead target observation. In what follows, we focus on impulse response analysis.

In an impulse response analysis, we seek to infer a smooth function $f_z(h)$ that represents an impulse response of y to z , namely, $f_z(h) = \partial y_{t+h} / \partial z_t$. Here, we allow a sequence $\{\beta_{(h_1)}, \dots, \beta_{(h_H)}\}$ to represent an impulse response of y to z , namely, $\beta_{(h)} = \partial y_{t+h} / \partial z_t$. The model can be represented as

$$\begin{aligned} y_{(h),t+h} &= \mathbf{x}_t^\top \boldsymbol{\theta}_{(h)} + u_{(h),t+h}, \quad t = 1, \dots, T; \quad h \in \mathcal{H}, \\ \mathbf{x}_t &= (z_t, 1, w_{1,t}, \dots, w_{J-2,t})^\top, \\ \boldsymbol{\theta}_{(h)} &= (\beta_{(h)}, \alpha_{(h)}, \gamma_{(h),1}, \dots, \gamma_{(h),J-2})^\top, \end{aligned}$$

where \mathbf{x}_t is a vector of regressors and $\boldsymbol{\theta}_{(h)}$ is a vector of corresponding parameters. For notational convenience, we reindex the coefficient vector as $\boldsymbol{\theta}_{(h)} = (\theta_{(h),1}, \dots, \theta_{(h),J})^\top$. Stacking these over the projection dimension yields a representation resembling a seemingly unrelated regression (SUR): for $t = 1, \dots, T$,

$$\begin{aligned}\mathbf{y}_t &= (\mathbf{I}_H \otimes \mathbf{x}_t^\top) \boldsymbol{\theta} + \mathbf{u}_t, \\ \mathbf{y}_t &= (y_{(h_1),t+h_1}, \dots, y_{(h_H),t+h_H})^\top, \quad \mathbf{u}_t = (u_{(h_1),t+h_1}, \dots, u_{(h_H),t+h_H})^\top, \\ \boldsymbol{\theta} &= (\boldsymbol{\theta}_{(h_1)}^\top, \dots, \boldsymbol{\theta}_{(h_H)}^\top)^\top,\end{aligned}$$

where \otimes denotes the Kronecker product.

Rearranging the above representation, we express the model in matrix notation as

$$\mathbf{y} = (\mathbf{I}_H \otimes \mathbf{X}) \boldsymbol{\theta} + \mathbf{u}, \quad \mathbf{u} \sim \mathcal{N}(\mathbf{0}_{HT}, \boldsymbol{\Sigma} \otimes \mathbf{I}_T) \quad (1)$$

$$\mathbf{y} = (\mathbf{y}_1^\top, \dots, \mathbf{y}_T^\top)^\top, \quad \mathbf{X} = (\mathbf{x}_1, \dots, \mathbf{x}_T)^\top, \quad \mathbf{u} = (\mathbf{u}_1^\top, \dots, \mathbf{u}_T^\top)^\top.$$

where $\boldsymbol{\Sigma}$ is a covariance matrix, and $\mathcal{N}(\mathbf{d}, \mathbf{B})$ denotes a multivariate normal distribution with mean \mathbf{d} and covariance \mathbf{B} . Letting \mathcal{D} denote the data, the likelihood takes a standard form:

$$\begin{aligned}p(\mathcal{D}|\boldsymbol{\theta}, \boldsymbol{\Sigma}) &= (2\pi)^{-\frac{HT}{2}} |\boldsymbol{\Sigma}|^{-\frac{T}{2}} \exp \left[-\frac{1}{2} \tilde{\mathbf{u}}^\top (\boldsymbol{\Sigma}^{-1} \otimes \mathbf{I}_T) \tilde{\mathbf{u}} \right] \\ &= (2\pi)^{-\frac{HT}{2}} |\boldsymbol{\Sigma}|^{-\frac{T}{2}} \exp \left[-\frac{1}{2} \text{tr} \left(\tilde{\mathbf{U}}^\top \tilde{\mathbf{U}} \boldsymbol{\Sigma}^{-1} \right) \right],\end{aligned}$$

$$\tilde{\mathbf{u}} = (\tilde{\mathbf{u}}_{(h_1)}^\top, \dots, \tilde{\mathbf{u}}_{(h_H)}^\top)^\top = \mathbf{y} - (\mathbf{I}_H \otimes \mathbf{X}) \boldsymbol{\theta},$$

where $\tilde{\mathbf{U}} = (\tilde{\mathbf{u}}_{(h_1)}, \dots, \tilde{\mathbf{u}}_{(h_H)})$ is a matrix composed of the realized residuals.

2.1.2 Bayesian Inference

This section first discusses priors on the subsets of $\boldsymbol{\theta}$ and then assembles them into a prior on $\boldsymbol{\theta}$, followed by a description of the priors on the other parameters. Lastly, the posterior simulation method is discussed.

We introduce a class of roughness penalty priors for $\boldsymbol{\theta}_j$, $j = 1, \dots, J$. Our prior construction is motivated by Lang and Brezger (2004). The prior induces an r th-order random-walk behavior on a sequence of parameters $\theta_{(h_1),j}, \dots, \theta_{(h_H),j}$. When $r = 2$, the relationship between $\theta_{(h_i),j}$ and successive parameters is represented by

$$\theta_{(h_i),j} = 2\theta_{(h_{i-1}),j} - \theta_{(h_{i-2}),j} + \epsilon_i, \quad \epsilon_i \sim \mathcal{N}\left(0, \tau_j^{-1} \lambda_{(h_i),j}^{-1}\right),$$

for $i = r+1, \dots, H$, where τ_j and $\lambda_{(h_i),j}$ are global and local smoothing parameters, respectively. Controlling local smoothness is potentially beneficial, because impulse response functions often have both strongly bent and smooth areas: for example, fast-growing responses immediately after an occurrence of shock and virtually flat responses after convergence to a long-run equilibrium. In some applications, without the adaptation for local smoothness, an estimated impulse response might be oversmoothed in some areas and undersmoothed in others. A prior on $\boldsymbol{\theta}_j$ is an improper normal prior generated by an intrinsic Gaussian Markov random field (Rue and Held, 2005), and the smoothing parameters are inferred from gamma priors, unlike in existing

approaches such as Miranda-Agrrippino and Ricco (2017); Barnichon and Matthes (2019). The hierarchy of the prior takes the form

$$\begin{aligned}
p(\boldsymbol{\theta}_j | \tau_j, \boldsymbol{\Lambda}_j) &\propto \exp \left[-\frac{\tau_j}{2} \sum_{i=r+1}^H \lambda_{(h_i),j} (\Delta^r \theta_{(h_i),j})^2 \right] \\
&= \exp \left(-\frac{\tau_j}{2} \boldsymbol{\theta}_j^\top \mathbf{D}^\top \boldsymbol{\Lambda}_j \mathbf{D} \boldsymbol{\theta}_j \right) \\
&= \exp \left(-\frac{\tau_j}{2} \boldsymbol{\theta}_j^\top \mathbf{Q}_j \boldsymbol{\theta}_j \right), \\
\lambda_{(h_{r+1}),j} &= 1 \text{ and } \lambda_{(h_i),j} \sim \mathcal{G}(\eta_1, \eta_2), \quad i = r+2, \dots, H, \\
\tau_j &\sim \mathcal{G}(\nu_1, \nu_2),
\end{aligned}$$

where $\boldsymbol{\Lambda}_j = \text{diag}(\lambda_{(h_{r+1}),j}, \dots, \lambda_{(h_H),j})$, \mathbf{D} is an $(H-r)$ -by- H difference matrix of order r , η_1 , η_2 , ν_1 , and ν_2 are pre-fixed hyperparameters, $\mathcal{G}(a, b)$ denotes a gamma distribution with shape a and rate b (and, thus, with mean a/b and variance a/b^2), and Δ^r denotes the r th-order difference operator. By assembling the priors on the subsets of $\boldsymbol{\theta}$, the prior density for $\boldsymbol{\theta}$ conditional on $\boldsymbol{\tau} = \{\tau_1, \dots, \tau_J\}$ and $\boldsymbol{\Lambda} = \{\boldsymbol{\Lambda}_1, \dots, \boldsymbol{\Lambda}_J\}$ is represented as

$$\begin{aligned}
p(\boldsymbol{\theta} | \boldsymbol{\tau}, \boldsymbol{\Lambda}) &\propto \exp \left(-\frac{1}{2} \boldsymbol{\theta}^\top \mathbf{Q} \boldsymbol{\theta} \right), \\
\mathbf{Q} &= \sum_{j=1}^J ((\tau_j \mathbf{D}^\top \boldsymbol{\Lambda}_j \mathbf{D}) \otimes \mathbf{E}_j), \tag{2}
\end{aligned}$$

where \mathbf{E}_j is a J -by- J zero matrix in which the j th diagonal element is replaced by one. In what follows, the above prior is referred to as an adaptive roughness penalty (A-RP) prior. As a special case, the same prior with all local smoothing parameters set to one is called a non-adaptive roughness penalty (N-RP) prior. For the N-RP prior, (2) can be rewritten as

$$\mathbf{Q} = \mathbf{D}^\top \mathbf{D} \otimes \text{diag}(\tau_1, \dots, \tau_J).$$

Choosing a prior of the covariance matrix $\boldsymbol{\Sigma}$ is non-trivial. Because of the strong correlations between the residuals, $\boldsymbol{\Sigma}$ tends to be close to a matrix of ones and almost singular. If the Jeffreys prior, a popular non-informative prior for covariance matrices, is employed, a posterior simulation easily crashes due to the singularity of the gram matrix of the realized residuals.² Therefore, prior-induced shrinkage is necessary to complete a posterior simulation. On the other hand, as Alvarez et al. (2014) argue, an inverse Wishart prior, another popular choice, can be unintentionally, significantly informative, resulting in significant biases. For these reasons, we use a hierarchical inverse Wishart (HIW) prior for $\boldsymbol{\Sigma}$ (Huang and Wand, 2013):

$$\begin{aligned}
\boldsymbol{\Sigma} | \boldsymbol{\Phi} &\sim \mathcal{IW}(2\zeta \boldsymbol{\Phi}, \zeta + H - 1), \\
\boldsymbol{\Phi} &= \text{diag}(\phi_{(h_1)}, \dots, \phi_{(h_H)}), \\
\phi_{(h_i)} &\sim \mathcal{G}\left(\frac{1}{2}, \nu\right), \quad i = 1, \dots, H,
\end{aligned}$$

²Bayesian inference using the Jeffreys prior for $\boldsymbol{\Sigma}$ almost always fails for the synthetic and real data used in the subsequent section.

Algorithm 1 Sampling θ (Rue 2001)

$$\theta \sim \mathcal{N}(\mathbf{m}, \mathbf{P}^{-1}),$$

$$\mathbf{m} = \mathbf{P}^{-1} (\boldsymbol{\Sigma}^{-1} \otimes \mathbf{X}^\top) \mathbf{y}, \quad \mathbf{P} = \boldsymbol{\Sigma}^{-1} \otimes \mathbf{X}^\top \mathbf{X} + \mathbf{Q} = \mathbf{L}\mathbf{L}^\top.$$

Step 1. Sample $\mathbf{a} \sim \mathcal{N}(\mathbf{0}_{HJ}, \mathbf{I}_{HJ})$.

Step 2. Solve $\mathbf{L}^\top \mathbf{b} = \mathbf{a}$ to obtain \mathbf{b} .

Step 3. Solve $\mathbf{L}\mathbf{c} = (\boldsymbol{\Sigma}^{-1} \otimes \mathbf{X}^\top) \mathbf{y}$ to obtain \mathbf{c} .

Step 4. Solve $\mathbf{L}^\top \mathbf{m} = \mathbf{c}$ to obtain \mathbf{m} .

Step 5. Set $\theta = \mathbf{b} + \mathbf{m}$.

where $\phi_{(h_i)}$ is a hyperparameter to be inferred, ζ and ν are prefixed hyperparameters, and $\mathcal{IW}(\mathbf{A}, b)$ is an inverse Wishart distribution with scale matrix \mathbf{A} and degrees of freedom b . This prior distribution is seen as a scale mixture of inverse Wishart distributions, and is more robust than an inverse Wishart prior. We conducted a simulation study that compares an inverse Wishart prior and the HIW prior and show that the HIW prior has better finite sample performance than an inverse Wishart prior. See Section A.1 in the ‘‘Online Appendix’’ for details.

We can induce this prior arbitrarily non-informative by setting ν to a very small value, but Huang and Wand’s (2013) recommendation $\nu = 10^{-10}$ (in our notation) is too flat to complete the posterior simulation in this paper. Our default choice in this paper is $\nu = 0.01$. Although there is no general procedure to find a sufficiently small value of ν , the results in the subsequent sections are not sensitive to ν as long as it is chosen from a fairly large range $[10^{-4}, 10^{-1}]$ (see Section A.2 in the ‘‘Online Appendix’’).

As demonstrated in Section A.2 in the Appendix, the proposed approach is not very sensitive to the choice of the hyperparameters. However, as the priors used in this paper are not scale-invariant, a user of the proposed approach is strongly encouraged to conduct a prior sensitivity check.

A posterior simulation is conducted using the Markov chain Monte Carlo (MCMC) algorithm. Because all of the conditional posterior densities are standard, we can construct a block Gibbs sampler. Each sampling block is specified as follows.

Sampling θ The conditional posterior density of θ is given by the multivariate normal distribution:

$$\theta|-\sim \mathcal{N}(\mathbf{m}, \mathbf{P}^{-1}),$$

$$\mathbf{m} = \mathbf{P}^{-1} (\boldsymbol{\Sigma}^{-1} \otimes \mathbf{X}^\top) \mathbf{y}, \tag{3}$$

$$\mathbf{P} = \boldsymbol{\Sigma}^{-1} \otimes \mathbf{X}^\top \mathbf{X} + \mathbf{Q}. \tag{4}$$

This block is computationally demanding, with two bottlenecks. The first is concerned with calculation of the prior precision matrix, which involves repeated high-dimensional matrix multiplications, Eq. (2). The computational cost declines significantly by treating \mathbf{Q} as a sparse matrix. The second bottleneck is the inversion of \mathbf{P} . For speed and numerical stability, we apply the algorithm described in Section 2 of Rue (2001) (see Algorithm 1), which exploits a banded structure of \mathbf{P} ; inverting a lower-triangular Cholesky root of \mathbf{P} , (denoted by \mathbf{L}), is faster and more numerically stable than inverting \mathbf{P} itself.

Sampling τ and Λ The conditional posteriors of the smoothing parameters for θ_j , $j = 1, \dots, J$, are specified as the following gamma distributions: for $j = 1, \dots, J$,

$$\begin{aligned}\tau_j | - &\sim \mathcal{G} \left(\nu_1 + \frac{1}{2} \text{rank}(\mathbf{D}^\top \mathbf{D}), \nu_2 + \frac{1}{2} \boldsymbol{\theta}_j^\top \mathbf{D}^\top \boldsymbol{\Lambda}_j \mathbf{D} \boldsymbol{\theta}_j \right), \\ \lambda_{(h_i),j} | - &\sim \mathcal{G} \left(\eta_1 + \frac{1}{2}, \eta_2 + \frac{\tau_j}{2} (\Delta^r \theta_{(h_i),j})^2 \right), \quad i = r + 2, \dots, H.\end{aligned}$$

Sampling Σ and Φ The conditional posteriors of Σ and Φ are

$$\begin{aligned}\Sigma | - &\sim \mathcal{IW} \left(2\zeta \Phi + \tilde{\mathbf{U}}^\top \tilde{\mathbf{U}}, \zeta + H - 1 + T \right), \\ \phi_{(h_i)} | - &\sim \mathcal{G} \left(\frac{\zeta + T}{2}, v + \zeta (\Sigma^{-1})_{i,i} \right), \quad i = 1, \dots, H,\end{aligned}$$

where $(\Sigma^{-1})_{i,i'}$ denotes the (i, i') -element of Σ^{-1} .

2.2 Local projection with B-spline expansions

We consider a local projection with B-spline expansions as an additional smoothing device. We intend to approximate an impulse response function $f_z(h)$ using a B-spline basis function expansion over a projection horizon³

$$f_z(h) = \beta_{(h)} \approx \sum_{k=1}^K b_k \varphi_k(h) = \mathbf{b}^\top \boldsymbol{\varphi}(h),$$

where K is a number of knots, $\mathbf{b} = (b_1, \dots, b_K)^\top$ is a vector of coefficients, and $\boldsymbol{\varphi}(h) = (\varphi_1(h), \dots, \varphi_K(h))^\top$ is a vector of B-spline basis functions. We define the approximations of the other coefficients in a similar fashion. Given the approximation, the model is represented as

$$\begin{aligned}y_{t+h} &\approx \sum_{k=1}^K a_k \varphi_k(h) + \sum_{k=1}^K b_k \varphi_k(h) z_t + \sum_{j=1}^{J-2} \sum_{k=1}^K c_{j,k} \varphi_k(h) w_{j,t} + u_{(h),t+h} \\ &= \mathbf{a}^\top \boldsymbol{\varphi}(h) + \mathbf{b}^\top \boldsymbol{\varphi}(h) z_t + \sum_{j=1}^{J-2} \mathbf{c}_j^\top \boldsymbol{\varphi}(h) w_{j,t} + u_{(h),t+h} \\ &= \boldsymbol{\vartheta}^\top (\tilde{\mathbf{x}}_t \otimes \boldsymbol{\varphi}(h)) + u_{(h),t+h},\end{aligned}$$

where $\tilde{\mathbf{x}}_t = (z_t, 1, w_{1,t}, \dots, w_{J-2,t})^\top$ is a vector of regressors, and $\boldsymbol{\vartheta} = (\mathbf{b}^\top, \mathbf{a}^\top, \mathbf{c}_1^\top, \dots, \mathbf{c}_{J-2}^\top)^\top$ is a vector of corresponding parameters. We reindex $\boldsymbol{\vartheta} = (\boldsymbol{\vartheta}_1^\top, \dots, \boldsymbol{\vartheta}_J^\top)^\top$ for expositional convenience. Letting $\tilde{\mathbf{x}}_{(h),t} = \tilde{\mathbf{x}}_t \otimes \boldsymbol{\varphi}(h)$, the model can be expressed as

$$y_{t+h} \approx \boldsymbol{\vartheta}^\top \tilde{\mathbf{x}}_{(h),t} + u_{(h),t+h}.$$

Stacking these equations over the projection dimension yields a representation à la SUR:

$$\mathbf{y}_t = \tilde{\mathbf{X}}_t \boldsymbol{\vartheta} + \mathbf{u}_t,$$

³See, for example, De Boor (1978); Eilers and Marx (1996) for a detailed description of B-splines.

$\mathbf{y}_t = (y_{t+h_1}, \dots, y_{t+h_H})^\top$, $\tilde{\mathbf{X}}_t = (\tilde{\mathbf{x}}_{(h_1),t}, \dots, \tilde{\mathbf{x}}_{(h_H),t})^\top$, $\mathbf{u}_t = (u_{(h_1),t+h_1}, \dots, u_{(h_H),t+h_H})^\top$,
for $t = 1, \dots, T$. Rearranging the above representation delivers

$$\begin{aligned} \mathbf{y} &= \tilde{\mathbf{X}}\boldsymbol{\vartheta} + \mathbf{u}, \quad \mathbf{u} \sim \mathcal{N}(\mathbf{0}_{HT}, \boldsymbol{\Sigma} \otimes \mathbf{I}_T), \\ \mathbf{y} &= \left(\mathbf{y}_{(h_1)}^\top \cdots \mathbf{y}_{(h_H)}^\top \right)^\top, \quad \tilde{\mathbf{X}} = \left(\tilde{\mathbf{X}}_{(h_1)}^\top \cdots \tilde{\mathbf{X}}_{(h_H)}^\top \right)^\top, \quad \mathbf{u} = \left(\mathbf{u}_{(h_1)}^\top, \dots, \mathbf{u}_{(h_H)}^\top \right)^\top, \\ \mathbf{y}_{(h)} &= \left(y_{(h),1} \cdots y_{(h),T} \right)^\top, \quad \tilde{\mathbf{X}}_{(h)} = \left(\tilde{\mathbf{x}}_{(h),1} \cdots \tilde{\mathbf{x}}_{(h),T} \right)^\top, \quad h \in \mathcal{H}, \\ \mathbf{u}_{(h)} &= \left(u_{(h),1}, \dots, u_{(h),T} \right)^\top, \quad h \in \mathcal{H}. \end{aligned} \tag{5}$$

We construct a posterior simulator for the model in a similar fashion as the model without B-spline expansions. Given the same priors for $\boldsymbol{\tau}$ and $\boldsymbol{\Lambda}$, a prior on $\boldsymbol{\vartheta}$ is constructed as

$$\begin{aligned} p(\boldsymbol{\vartheta} | \boldsymbol{\tau}, \boldsymbol{\Lambda}) &\propto \exp\left(-\frac{1}{2}\boldsymbol{\vartheta}^\top \mathbf{Q}\boldsymbol{\vartheta}\right), \\ \mathbf{Q} &= \text{blkdiag}\left(\tau_1 \mathbf{D}^\top \boldsymbol{\Lambda}_1 \mathbf{D}, \dots, \tau_J \mathbf{D}^\top \boldsymbol{\Lambda}_J \mathbf{D}\right). \end{aligned} \tag{6}$$

The conditional posterior density of $\boldsymbol{\vartheta}$ is derived as the multivariate normal distribution

$$\begin{aligned} \boldsymbol{\vartheta} | - &\sim \mathcal{N}(\mathbf{m}, \mathbf{P}^{-1}), \\ \mathbf{m} &= \mathbf{P}^{-1} \tilde{\mathbf{X}}^\top (\boldsymbol{\Sigma}^{-1} \otimes \mathbf{I}_T) \mathbf{y}, \\ \mathbf{P} &= \mathbf{Q} + \tilde{\mathbf{X}}^\top (\boldsymbol{\Sigma}^{-1} \otimes \mathbf{I}_T) \tilde{\mathbf{X}}. \end{aligned} \tag{7}$$

As in the model without B-spline expansions, this sampling block presents a major computational burden. On the one hand, the prior precision matrix \mathbf{Q} can be calculated easily by virtue of its block diagonal structure (6) (unless the number of covariates J is not extremely large). On the other hand, the quantity $\tilde{\mathbf{X}}^\top (\boldsymbol{\Sigma}^{-1} \otimes \mathbf{I}_T) \tilde{\mathbf{X}}$ in (7) involves a high-dimensional matrix multiplication and cannot be compressed as in (4), eventually making the posterior simulation more demanding than the previous case. Sampling distributions of the other parameters are derived analogously to those of a model without B-spline expansions.

3 Simulation Study

We conducted Monte Carlo simulations to investigate the performance of our proposed approach. We considered six specifications consisting of the combination of three priors, each with/without B-spline expansions. As with the N-RP and A-RP priors, we considered a weakly informative independent standard normal prior, $\boldsymbol{\theta} \sim \mathcal{N}(\mathbf{0}, 10^4 \mathbf{I})$.

First, we considered a linear data generating processes (DGPs) specified by the following moving average representation:

$$\begin{aligned} y_t &= \sum_{l=0}^L \beta_{(l)} z_{t-l} + \epsilon_t, \\ z_t &\sim \mathcal{N}(0, 1), \quad \epsilon_t \sim \mathcal{N}(0, 1), \end{aligned}$$

where y_t is an endogenous variable, z_t is an exogenous variable, and ϵ_t is the measurement error. A set of parameters $\beta_{(0)}, \dots, \beta_{(L)}$ represents an impulse response. True parameter values are defined as a convex curve:

$$\beta_{(l)} = \frac{l \exp(r(1-l))}{\sum_{l'=0}^L l' \exp(r(1-l'))},$$

$$r \sim \mathcal{U}(0.1, 1),$$

where $\mathcal{U}(0.1, 1)$ denotes a uniform distribution with support $(0.1, 1)$, and r governs where the peak of the impulse response is located. Covariates are a constant and four lags of y_t and z_t . We fixed the length of the impulse response to $L = 20$ and the effective sample size to $T = 50, 100$. Hyperparameters are $\nu = \nu_1 = \nu_2 = 0.01$, $\eta = \eta_1 = \eta_2 = 0.5$, and $v = 0.01$. We choose the order of the difference matrix as $r = 2$, implying that the sequences of parameters to be inferred are induced to straight lines. We use the B-spline basis with equidistant knots ranging from $h_1 - 2$ to $h_H - 1$ with unitary increments. We set the degree of the B-spline bases to three. We generate 500 sets of synthetic data. Gibbs sampling obtained 40,000 posterior draws, after discarding the initial 10,000. Each chain is initialized to an ordinary least squares estimate.

We compared the alternative approaches on the basis of four performance measures: mean squared errors (MSE), coverage probability (Coverage), lengths of credible intervals (Length), and computational speed (Speed). MSE is the sum of mean squared errors,

$$\text{MSE} = M^{-1} \sum_{m=1}^M \sum_{l=0}^L \left(\hat{\beta}_{m,(l)} - \beta_{m,(l)}^{true} \right)^2,$$

where $\hat{\beta}_{m,(l)}$ denotes a posterior mean estimate of $\beta_{(l)}$ in the m th experiment, $\beta_{m,(l)}^{true}$ denotes the corresponding true value, and M is a total number of experiments. Coverage is the arithmetic mean of the probability that the true value is within the 90% credible interval:

$$\text{Coverage} = M^{-1} L^{-1} \sum_{m=1}^M \sum_{l=0}^L \mathbf{1}_{\{\hat{\beta}_{m,(l)}^{5\%} < \beta_{m,(l)}^{true}\}} \times \mathbf{1}_{\{\hat{\beta}_{m,(l)}^{95\%} > \beta_{m,(l)}^{true}\}},$$

where $\hat{\beta}_{m,(l)}^{5\%}$ and $\hat{\beta}_{m,(l)}^{95\%}$ are posterior 5th and 95th percentile estimates of $\beta_{(l)}$ in the m th experiment. Length denotes the arithmetic mean of the lengths of a 90% credible interval,

$$\text{Length} = M^{-1} L^{-1} \sum_{m=1}^M \sum_{l=0}^L \left(\hat{\beta}_{m,(l)}^{95\%} - \hat{\beta}_{m,(l)}^{5\%} \right).$$

Speed is the mean computational time of posterior simulations in seconds.⁴

Table 1 reports results of the first experiment. With regard to MSE and Length, the N-RP and A-RP priors outperform the normal prior, while the A-RP prior performs slightly worse than the N-RP prior. Using B-spline expansions reduces MSE and Length but the magnitude is tiny. Use of the prior and the B-spline does not reduce Coverage. Speed depends on the prior specification and on whether a B-spline is used. The difference attributable to the choice of prior is not notably large, but the use of a B-spline imposes a significant computational burden. When B-spline expansions are employed, approximately 95% of computational time during

⁴All programs were written in Matlab 2016a (64 bit) and executed on an Ubuntu Desktop 16.04 LTS (64 bit), running on Intel Xeon E5-2607 v3 processors (2.6GHz).

each MCMC cycle is spent calculating \mathbf{P} , in particular, a quantity $\tilde{\mathbf{X}}^\top (\boldsymbol{\Sigma}^{-1} \otimes \mathbf{I}_T) \tilde{\mathbf{X}}$. This bottleneck is a simple matrix-matrix multiplication that is executed via a built-in mathematical routine of Matlab, so switching to a compiled language such as Fortran and C/C++ will not totally resolve the problem. We checked the sensitivity of the simulation results to choice of the hyperparameters. The results are summarized in the ‘‘Online Appendix’’.

That the B-spline function expansions have only a marginal effect is not surprising, given that response variables can appear as functional data observed on an equally spaced grid.⁵ Panel (a) in Figure 1 displays B-spline basis functions on a fine grid (2,401 points) and simulated functional data. This situation is presumed in a functional data analysis. In a local projection, however, observation points ($h \in \mathcal{H}$) are sparse and invariant, as demonstrated in panel (b). As is evident from there, B-spline expansions merely allocate observed information to the fixed grids, rather than interpolating neighboring information. In our case, observed information for a single grid point is allocated to neighboring grid points with weights $\{1/6, 3/2, 1/6\}$.⁶ Therefore, using a B-spline indeed smooths estimates of impulse responses, but its effectiveness is limited.

We fortified our results by considering nonlinear DGPs characterized by asymmetric and state-dependent impulse responses, respectively. The asymmetric DGP is specified by

$$y_t = \sum_{l=0}^L \left(\beta_{(l)}^{[1]} z_{t-l} \mathbf{1}_{\{z_{t-l} < 0\}} + \beta_{(l)}^{[2]} z_{t-l} \mathbf{1}_{\{z_{t-l} \geq 0\}} \right) + \epsilon_t,$$

while the state-dependent DGP is specified by

$$y_t = \sum_{l=0}^L \left(\beta_{(l)}^{[1]} z_{t-l} \mathbf{1}_{\{y_{t-l} < 0\}} + \beta_{(l)}^{[2]} z_{t-l} \mathbf{1}_{\{y_{t-l} \geq 0\}} \right) + \epsilon_t,$$

where $\mathbf{1}_{\{\cdot\}}$ denotes the indicator function. For both cases, two sets of parameters are independently generated in the same way as the linear DGP. We set $T = 80, 160$. The other settings are exactly the same as those in the first experiment. For computational reasons, we did not consider a model with B-spline expansions. Table 2 presents the results, in which we largely verified the result of the first experiment. With regard to MSE and Length, the N-RP and A-RP priors consistently improve accuracy versus the normal prior. Coverage values obtained using the N-RP and A-RP priors are slightly smaller than those using the normal prior.

From the simulation study, we obtained two findings. First, our proposed approach improves the finite sample performance of local projection, while such improvements are almost entirely attributable to the roughness penalty priors and not to the B-spline expansions. Second, despite its flexibility, the A-RP prior is not superior to the N-RP prior. In conclusion, a specification with the N-RP prior and no B-spline expansion is recommendable as a first choice.

4 Application

To demonstrate our model, we applied our approach to an analysis of monetary policy in the United States. We use monetary policy shocks compiled by Coibion et al. (2017) which is an

⁵From this point of view, local projections are similar to functional data models such as Guo (2002); Morris and Carroll (2006).

⁶When the degree of the B-spline bases is increased to 5, the weight set becomes $\{1/120, 13/60, 33/60, 13/60, 1/120\}$. The added weights are too small to affect the estimate ($1/120 \approx 0.0083$).

update of Romer and Romer (2004).⁷ For the covariates and the response, we considered the following three macroeconomic variables, downloaded from the Federal Reserve Economic Data (FRED), maintained by the Federal Reserve Bank of St. Louis: the industrial production index (FRED mnemonic: INDPRO), the consumer price index for all urban consumers: all items (CPIAUCSL), and the effective federal funds rate (FEDFUNDS). We also treated all three as response variables. We included lags of monetary policy shock as covariates. All data are monthly and spans from March 1969 to December 2008. The range is limited by the availability of data for monetary policy shocks. Industrial production and the inflation rate are seasonally adjusted, and included as annualized month-to-month percentage changes (log-difference multiplied by 1,200). We included the time trend and up to four lags of covariates. We choose hyperparameters as in the previous section. The Gibbs sampler obtained a total of 40,000 posterior draws after discarding the first 10,000.

Figures 2, 3, and 4 show posterior estimates of the impulse responses of the macroeconomic variables to monetary policy shocks under different specifications.⁸ The shaded areas indicate the 90% credible sets for a preferred specification using no B-spline and the N-RP prior. For all the response variables, the roughness penalty priors successfully penalize the roughness of the impulse response functions. Thus, we obtain economically plausible, smoothed estimates, and can interpret the shape of the impulse response easily, recognizing the underlining response. Use of the B-spline exerts no significant effect on the shape of the impulse response.

We then compared the fitness of these estimates based on the deviance information criterion (DIC) (Spiegelhalter et al., 2002) and the Watanabe–Akaike information criterion (WAIC) (Watanabe, 2010). Table 3 reports on both criteria for different specifications (reported values are on the deviance scale; the smaller, the better). Specifications including the roughness penalty priors outperform the normal prior in predictive accuracy regardless of the fitness measure, while the use of a B-spline yields only limited improvement. Both B-spline and the roughness penalty prior enhance fitness, but almost all improvements originate from the latter.⁹ This finding supports our simulation results. When the B-spline is not used, the posterior simulation takes 26 minutes to generate 50,000 draws; when it is used, the same simulation takes 66 hours. Considering the higher computational cost, use of a B-spline would not be out of proportion to the benefit for many applications (Table 3).

5 Comparison with Existing Approaches

Recent frequentist approaches to estimate smooth impulse response are closely related to ours in that their objective functions have forms similar to the posterior densities we present, i.e., the sum of a log Gaussian likelihood and a penalty term. From this perspective, Barnichon and

⁷The time series of monetary policy shocks is from Yuriy Gorodnichenko’s website (<https://eml.berkeley.edu/~ygorodni/index.htm>).

⁸In the “Online Appendix”, Figs. A.1, A.2, and A.3 display credible intervals for all the specifications.

⁹Both the DIC and WAIC are asymptotically related to the AIC. Thus, one might consider evaluating the statistical significance of the difference in the values of the criteria of two models by applying a rule of thumb that is originally proposed to Bayes factor. As Burnham and Anderson (2004) describe, the AIC can be interpreted as an approximation of the log marginal likelihood of a model under a “savvy” prior that is a function of sample size and the number of model parameters. According to Jeffreys’s (1961) rule of thumb, the statistical significance of the difference between two models is “weak” if the difference in the AIC/DIC/WAIC is 0-2, “positive” if 2-6, “strong” if 6-10, or “very strong” if >10 (see also Raftery, 1995). When this rule of thumb is directly applied to Table 3, one might be able to interpret the results as follows: the statistical significance of the differences related to the prior choice is “very strong,” and the significance of the differences attributable to the use of B-splines is “weak” or “positive” when the Normal prior is used while it is “very strong” when the N-RP prior is used.

Brownlees (2019) can be seen as a frequentist counterpart to our approach with both B-spline expansions and roughness penalty priors. Their objective function is written in our notation as

$$\hat{\boldsymbol{\vartheta}} = \arg \min \left\| \mathbf{y} - \tilde{\mathbf{X}} \boldsymbol{\vartheta} \right\|^2 + \boldsymbol{\vartheta}^\top (\tilde{\tau} \mathbf{I}_J \otimes \mathbf{D}^\top \mathbf{D}) \boldsymbol{\vartheta}.$$

They propose to selecting a (scalar) smoothing parameter $\tilde{\tau}$ using a k -fold cross validation. Barnichon and Brownlees's (2019) approach bears only one smoothing parameter, rendering it less flexible than ours. Figures 5, 6, and 7 plot the posterior estimates of the (global) smoothing parameters for the real data considered in Section 4. As evident from these figures, the posterior estimates of the smoothing parameters are significantly different from covariate to covariate. Having single smoothing parameter seems implausible in practice.

El-Shagi's (2019) approach can be regarded as a frequentist version of a model using the N-RP priors and no B-spline expansion. His estimator is written in our notation as

$$\hat{\boldsymbol{\theta}} = \arg \min \left\| \mathbf{y} - \tilde{\mathbf{X}} \boldsymbol{\theta} \right\|^2 + \boldsymbol{\theta}^\top [\mathbf{D}^\top \mathbf{D} \otimes \text{diag}(\tau_1, \dots, \tau_J)] \boldsymbol{\theta}.$$

This boils down to a least squares estimator of $\boldsymbol{\theta}$ for an extended model specified by

$$\begin{pmatrix} \mathbf{y} \\ \mathbf{0}_{H-r} \end{pmatrix} = \begin{pmatrix} \mathbf{I}_H \otimes \mathbf{X} \\ \mathbf{D} \otimes \text{diag}(\tau_1^{1/2}, \dots, \tau_J^{1/2}) \end{pmatrix} \boldsymbol{\theta} + \begin{pmatrix} \mathbf{u} \\ \mathbf{u}^* \end{pmatrix},$$

where \mathbf{u}^* is an $(H - r)$ -dimensional vector of pseudo residuals generated by the penalty term. Let $\boldsymbol{\Sigma}^*$ denote the covariance matrix of \mathbf{u}^* . Given $\boldsymbol{\Sigma}$ and $\boldsymbol{\Sigma}^*$, a generalized least squares (GLS) estimator of $\boldsymbol{\theta}$ is

$$\begin{aligned} \hat{\boldsymbol{\theta}} &= \left[\boldsymbol{\Sigma}^{-1} \otimes (\mathbf{X}^\top \mathbf{X}) + \tilde{\mathbf{D}}^\top (\boldsymbol{\Sigma}^*)^{-1} \tilde{\mathbf{D}} \right]^{-1} (\boldsymbol{\Sigma}^{-1} \otimes \mathbf{X}^\top) \mathbf{y}, \\ \tilde{\mathbf{D}} &= \mathbf{D} \otimes \text{diag}(\tau_1^{1/2}, \dots, \tau_J^{1/2}). \end{aligned} \quad (8)$$

He chooses $r = 2$, restricts $\boldsymbol{\Sigma}$ to be diagonal and set $\boldsymbol{\Sigma}^*$ to a submatrix of $\boldsymbol{\Sigma}$, that is,

$$\boldsymbol{\Sigma} = \text{diag}(\sigma_{1,1}^2, \dots, \sigma_{H,H}^2), \quad \boldsymbol{\Sigma}^* = \text{diag}(\sigma_{2,2}^2, \dots, \sigma_{H-1,H-1}^2) \otimes \mathbf{I}_J.$$

As $\boldsymbol{\Sigma}$ is unknown, the parameters are estimated through a feasible GLS procedure. First, an ordinary least squares (OLS) estimate $\hat{\boldsymbol{\theta}}_{OLS}$ is obtained, and then $\hat{\boldsymbol{\Sigma}}_{OLS}$ is computed using the realized residuals. Second, using $\hat{\boldsymbol{\Sigma}}_{OLS}$, a first-stage GLS estimate $\hat{\boldsymbol{\theta}}_{GLS,1}$ is computed as (8) and compute $\hat{\boldsymbol{\Sigma}}_{GLS,1}$ using the obtained realized residuals. Lastly, using $\hat{\boldsymbol{\Sigma}}_{GLS,1}$, a second-stage (final) GLS estimate $\hat{\boldsymbol{\theta}} = \hat{\boldsymbol{\theta}}_{GLS,2}$ is obtained. He chooses $\boldsymbol{\tau} = \{\tau_1, \dots, \tau_J\}$ by minimizing the finite sample corrected Akaike's information criterion (AICc) (Hurvich et al., 1998),

$$AIC_c(\boldsymbol{\tau}) = -2 \log p \left(\mathcal{D} | \hat{\boldsymbol{\theta}}_{GLS,2}, \hat{\boldsymbol{\Sigma}}_{GLS,1} \right) + 2\delta + \frac{2\delta(\delta+1)}{T-\delta-1},$$

or a variant of the Bayesian information criterion (BICc) analogously defined as the AICc,

$$BIC_c(\boldsymbol{\tau}) = -2 \log p \left(\mathcal{D} | \hat{\boldsymbol{\theta}}_{GLS,2}, \hat{\boldsymbol{\Sigma}}_{GLS,1} \right) + (\log T) \delta + \frac{2\delta(\delta+1)}{T-\delta-1}.$$

δ denotes the effective loss of degrees of freedom (or pseudo dimension of the model) which is defined as the trace of a hat (or projection) matrix $\hat{\mathbf{P}}$ with $\hat{\mathbf{y}} = \hat{\mathbf{P}} \mathbf{y}$, that is, $\delta = \text{tr} \left\{ \hat{\mathbf{P}} \right\}$ with

$$\hat{P} = [\Sigma^{-1} \otimes (\mathbf{X}^\top \mathbf{X}) + (\mathbf{D}^\top (\Sigma^*)^{-1} \mathbf{D}) \otimes \text{diag}(\tau_1, \dots, \tau_J)]^{-1} [\Sigma^{-1} \otimes (\mathbf{X}^\top \mathbf{X})].$$

In terms of nonparametric regressions, δ measures the effective number of zero-th order polynomial bases defined over the projection horizons \mathcal{H} , $\mathbf{x}_t, \dots, \mathbf{x}_t$. This approach can be crudely interpreted as a maximum a posteriori estimation of a local projection using a (non-adaptive) roughness penalty prior of θ , a “prior” of τ generated from the AICc or BICc, and a non-informative prior of Σ . Figures 8, 9, and 10 represent estimated IRFs of monetary policy shocks using El-Shagi’s (2019) approach along with the default Bayesian estimates. The IRFs obtained by both approaches are fairly comparable.

We can identify three advantages of the proposed Bayesian approach over the frequentist approaches. First, our approach can provide credible intervals in a consistent and straightforward manner. In contrast, at this time, the frequentist approaches have no statistically grounded method to estimate confidence intervals; Barnichon and Brownlees (2019) mention a heuristic method, while El-Shagi (2019) does not discuss a method to estimate confidence intervals.

Second, while frequentist approaches fix smoothing parameters before inference by cross validation (Barnichon and Brownlees, 2019) or penalized optimization (El-Shagi, 2019), our approach infers them using priors, allowing us to systematically consider uncertainty in the smoothness of an impulse response (and other sequences of coefficients). The quantitative significance of this conceptual advantage depends on context. We re-estimated the model with the (global) smoothing parameters fixed to the posterior medians for the default specifications. As shown in Figure 11, for the real data in Section 5, there is no significant difference.

Third, the proposed approach has better finite-sample performance. We compared El-Shagi’s (2019) approach to ours through a simulation study. The simulation setup is the same as that of the linear IRF in Section 4.¹⁰ We examine specifications with unrestricted and diagonal covariance matrices for both El-Shagi’s (2019) and our Bayesian approaches. A half-t prior is used for the diagonal elements in Σ , denoted by $\sigma_{(h_i)}^2$, $i = 1, \dots, H$. It is derived from the HIW prior by setting $H = 1$:

$$\sigma_{(h_i)}^2 | \phi \sim \text{IG} \left(\frac{\zeta}{2}, \zeta \phi_{(h_i)} \right), \quad \phi_{(h_i)} \sim \mathcal{G} \left(\frac{1}{2}, v \right), \quad i = 1, \dots, H.$$

We choose $v = 0.01$ as in Section 3. The result is summarized in Table 4.¹¹ In line with the simulation study by El-Shagi (2019), finite sample performance of the BICc is comparable to or slightly better than the AICc. The Bayesian approach obtained smaller MSE on average than the FGLS approach for both covariance specifications. For the frequentist approach, specifications with diagonal covariances obtained smaller MSEs than those with unrestricted covariances, whereas for the Bayesian approach, the situation is the opposite. It is difficult to identify a specific reason behind this twisted simulation result. The plug-in estimator of Σ employed in the frequentist approach might not work well for the short time series.¹² The overall winner was the Bayesian approach with unrestricted covariance. Because residuals in a local projection are strongly correlated by construction, assuming independence between them is inappropriate.

¹⁰We minimize the information criteria using the limited-memory Broyden-Fletcher-Goldfarb-Shanno algorithm with bounds (Byrd et al., 1995), using a Matlab routine `minConf_TMP.m` written by Mark Schmidt. (<https://www.cs.ubc.ca/~schmidtm/Software/minConf.html>)

¹¹We also considered Jeffreys prior for $\sigma_{(h_i)}^2$ and obtained almost the same result for the half-t prior (thus, it is not reported).

¹²As T increases (e.g., $T = 500$), the relative performance of the FGLS approach with unrestricted covariance becomes comparable with that with diagonal covariance (not reported).

6 Conclusion

This study developed a fully Bayesian approach to estimate local projections using roughness penalty priors. It is also considered a specification involving a B-spline basis function expansion. Monte Carlo experiments have demonstrated that both B-splines and the roughness penalty priors improve statistical efficiency, however, almost all the improvements originate from the latter. Applying our proposed method to an analysis of monetary policy in the United States shows that the roughness penalty priors successfully smooth posterior estimates of the impulse response functions, and can improve the predictive accuracy of local projections.

This study addresses one of the two disadvantages of local projections, compared with the standard statistical framework that includes VAR, namely, that of less statistical efficiency. The other disadvantage that the exogenous variable is identified ex ante can be resolved by a two-stage regression approach, as in Aikman et al. (2016). Constructing a Bayesian counterpart to this line of approach has not been studied. In addition, it is potentially beneficial to develop more robust approaches than ours: for example, a choice of hyperparameters, heteroskedasticity and autocorrelations in errors, and so on. This study provides a first step for further developments of Bayesian local projections.

Acknowledgement The author would like to thank Professor Hideki Konishi for his guidance and encouragement. The author would also like to thank anonymous referees as well as participants at the Applied Statistics 2018 for their valuable suggestions and comments.

References

- Aikman, D., O. Bush, and A. M. Taylor (2016) “Monetary Versus Macroprudential Policies: Causal Impacts of Interest Rates and Credit Controls in the Era of the UK Radcliffe Report,” NBER Working Paper 22380.
- Alvarez, I., J. Niemi, and M. Simpson (2014) “Bayesian Inference for a Covariance Matrix,” in *26th Annual Conference on Applied Statistics in Agriculture*.
- Auerbach, A. J. and Y. Gorodnichenko (2013) “Fiscal Multipliers in Recession and Expansion,” in A. Alesina and F. Giavazzi eds. *Fiscal Policy after the Financial Crisis*: University of Chicago Press, 63–98.
- Barnichon, R. and C. Matthes (2019) “Functional Approximations of Impulse Responses,” *Journal of Monetary Economics*, Vol. 99, No. 1, 41–55.
- Barnichon, R. and C. Brownlees (2019) “Impulse Response Estimation By Smooth Local Projections,” *Review of Economics and Statistics*, Vol. 101, No. 3, 522–230.
- Burnham, K. P. and D. R. Anderson (2004) “Multimodel Inference: Understanding AIC and BIC in Model Selection,” *Sociological Methods & Research*, Vol. 33, No. 2, 261–304.
- Byrd, R. H., P. Lu, J. Nocedal, and C. Zhu (1995) “A Limited Memory Algorithm for Bound Constrained Optimization,” *SIAM Journal on Scientific Computing*, Vol. 16, No. 5, 1190–1208.
- Coibion, O., Y. Gorodnichenko, L. Kueng, and J. Silvia (2017) “Innocent Bystanders? Monetary Policy and Inequality,” *Journal of Monetary Economics*, Vol. 88, No. 1, 70–89.

- De Boor, C. (1978) *A Practical Guide to Splines*, Vol. 27: Springer-Verlag New York.
- Eilers, P. H. and B. D. Marx (1996) “Flexible Smoothing with B-splines and Penalties,” *Statistical Science*, Vol. 11, No. 2, 89–121.
- El-Shagi, M. (2019) “A Simple Estimator for Smooth Local Projections,” *Applied Economics Letters*, Vol. 26, No. 10, 830–834.
- Geweke, J. (2005) *Contemporary Bayesian Econometrics and Statistics*, Vol. 537: John Wiley & Sons.
- Guo, W. (2002) “Functional mixed effects models,” *Biometrics*, Vol. 58, No. 1, 121–128.
- Huang, A. and M. P. Wand (2013) “Simple Marginally Noninformative Prior Distributions for Covariance Matrices,” *Bayesian Analysis*, Vol. 8, No. 2, 439–452.
- Hurvich, C. M., J. S. Simonoff, and C.-L. Tsai (1998) “Smoothing Parameter Selection in Non-parametric Regression Using an Improved Akaike Information Criterion,” *Journal of the Royal Statistical Society: Series B (Statistical Methodology)*, Vol. 60, No. 2, 271–293.
- Jeffreys, H. (1961) *Theory of Probability*: Oxford University Press, 3rd edition.
- Jordà, Ò. (2005) “Estimation and Inference of Impulse Responses Local Projections,” *American Economic Review*, Vol. 95, No. 1, 161–182.
- Lang, S. and A. Brezger (2004) “Bayesian P-splines,” *Journal of Computational and Graphical Statistics*, Vol. 13, No. 1, 183–212.
- Miranda-Agrippino, S. and G. Ricco (2017) “The Transmission of Monetary Policy Shocks,” Staff Working Paper 657, Bank of England.
- Morris, J. S. and R. J. Carroll (2006) “Wavelet-based functional mixed models,” *Journal of the Royal Statistical Society: Series B (Statistical Methodology)*, Vol. 68, No. 2, 179–199.
- Raftery, A. E. (1995) “Bayesian Model Selection in Social Research,” *Sociological Methodology*, Vol. 25, 111–163.
- Ramey, V. A. (2016) “Macroeconomic Shocks and Their Propagation,” in J. B. Taylor and H. Uhlig eds. *Handbook of Macroeconomics*, Vol. 2A: Elsevier, Chap. 2, 71–162.
- Ramey, V. A. and S. Zubairy (2018) “Government Spending Multipliers in Good Times and in Bad: Evidence from U.S. Historical Data,” *Journal of Political Economy*, Vol. 126, No. 2, 850–901.
- Riera-Crichton, D., C. A. Vegh, and G. Vuletin (2015) “Procyclical and Countercyclical Fiscal Multipliers: Evidence from OECD Countries,” *Journal of International Money and Finance*, Vol. 52, 15–31.
- Romer, C. D. and D. H. Romer (2004) “A New Measure of Monetary Shocks: Derivation and Implications,” *American Economic Review*, Vol. 94, No. 1, 1055–1084.
- Rue, H. (2001) “Fast Sampling of Gaussian Markov Random Fields,” *Journal of the Royal Statistical Society, Series B*, Vol. 63, No. 2, 325–338.

- Rue, H. and L. Held (2005) *Gaussian Markov Random Fields: Theory and Applications*: CRC press.
- Spiegelhalter, D. J., N. G. Best, B. P. Carlin, and A. Van Der Linde (2002) “Bayesian Measures of Model Complexity and fit,” *Journal of the Royal Statistical Society, Series B*, Vol. 64, No. 4, 583–639.
- Stock, J. H. and M. W. Watson (2007) “Why Has US Inflation Become Harder to Forecast?” *Journal of Money, Credit and Banking*, Vol. 39, No. s1, 3–33.
- Watanabe, S. (2010) “Asymptotic Equivalence of Bayes Cross Validation and Widely Applicable Information Criterion in Singular Learning Theory,” *Journal of Machine Learning Research*, Vol. 11, No. Dec, 3571–3594.

Table 1: Results of the Monte Carlo simulation: linear IRF

T	Prior	B-spline	MSE	Length	Coverage	Speed
50	Normal		0.542	0.976	0.997	99
	Normal	✓	0.542	0.976	0.997	1174
	N-RP		0.131	0.432	0.994	105
	N-RP	✓	0.130	0.423	0.994	1164
	A-RP		0.150	0.468	0.994	120
	A-RP	✓	0.151	0.459	0.993	1167
100	Normal		0.243	0.599	0.995	150
	Normal	✓	0.243	0.599	0.995	4296
	N-RP		0.067	0.309	0.994	152
	N-RP	✓	0.067	0.301	0.991	4291
	A-RP		0.074	0.331	0.995	167
	A-RP	✓	0.074	0.323	0.993	4299

Note: MSE denotes the mean squared error. Coverage denotes the arithmetic mean of the probability that the true value is within a 90% credible interval. Length denotes the length of the 90% credible interval. Speed denotes computational time in seconds.

Table 2: Results of the Monte Carlo simulation: nonlinear IRF

T	DGP	Prior	MSE	Length	Coverage
80	Asymmetric	Normal	2.489	1.439	0.997
		N-RP	0.564	0.618	0.994
		A-RP	0.643	0.670	0.994
	State-dependent	Normal	1.526	1.073	0.996
		N-RP	0.453	0.500	0.985
		A-RP	0.504	0.541	0.987
160	Asymmetric	Normal	1.211	0.911	0.993
		N-RP	0.339	0.445	0.988
		A-RP	0.373	0.477	0.989
	State-dependent	Normal	0.648	0.666	0.993
		N-RP	0.216	0.355	0.986
		A-RP	0.234	0.380	0.989

Note: MSE denotes the mean squared error. Coverage denotes the arithmetic mean of the probability that the true value is within a 90% credible interval. Length denotes the length of the 90% credible interval.

Table 3: Comparison of fitness

(a) Industrial production	Normal prior		N-RP prior	
	DIC	WAIC	DIC	WAIC
without B-spline	32,585	31,894	31,872	31,431
with B-spline	32,583	31,894	31,854	31,423
(b) Inflation	Normal prior		N-RP prior	
	DIC	WAIC	DIC	WAIC
without B-spline	29,955	29,073	29,321	28,675
with B-spline	29,950	29,068	29,309	28,647
(c) Fed funds rate	Normal prior		N-RP prior	
	DIC	WAIC	DIC	WAIC
without B-spline	35,457	34,901	34,756	34,455
with B-spline	35,461	34,902	34,732	34,445

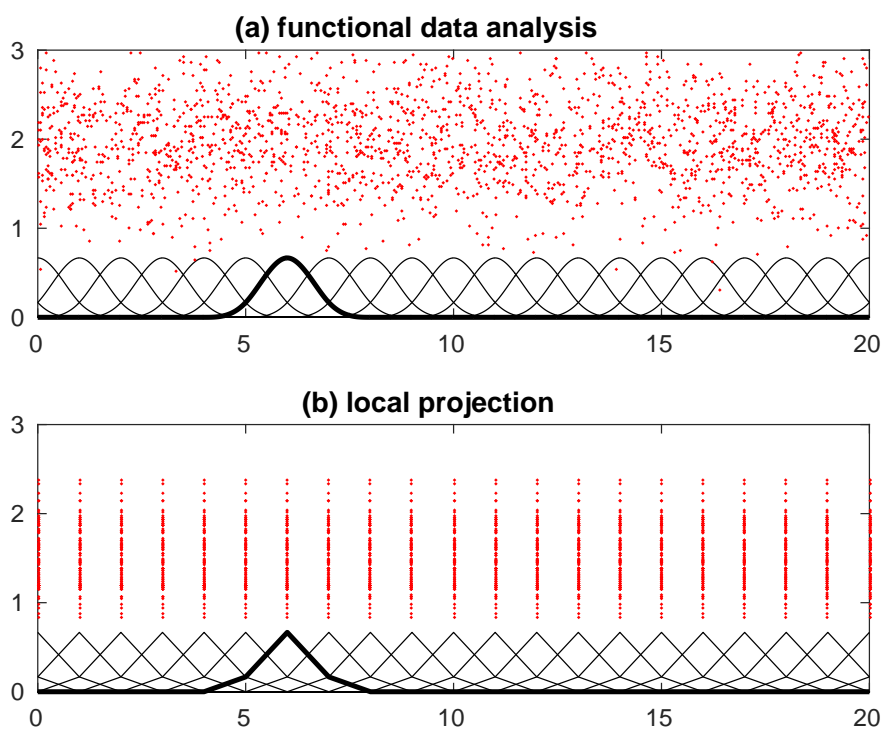
Note: Values of the DIC (deviance information criterion) and WAIC (Wanatabe-Akaike information criterion) under different specifications are reported. All values are on the deviance scale.

Table 4: Results of the Monte Carlo simulation: comparison to the frequentist approach

T	Prior	Penalty/Prior	MSE		Length		Coverage	
			full	diagonal	full	diagonal	full	diagonal
50	FGLS	AICc	0.221	0.162	–	–	–	–
		BICc	0.166	0.110	–	–	–	–
	Bayes	N-RP	0.131	0.151	0.432	0.298	0.994	0.925
100	FGLS	AICc	0.100	0.091	–	–	–	–
		BICc	0.100	0.091	–	–	–	–
	Bayes	N-RP	0.067	0.076	0.309	0.213	0.994	0.925

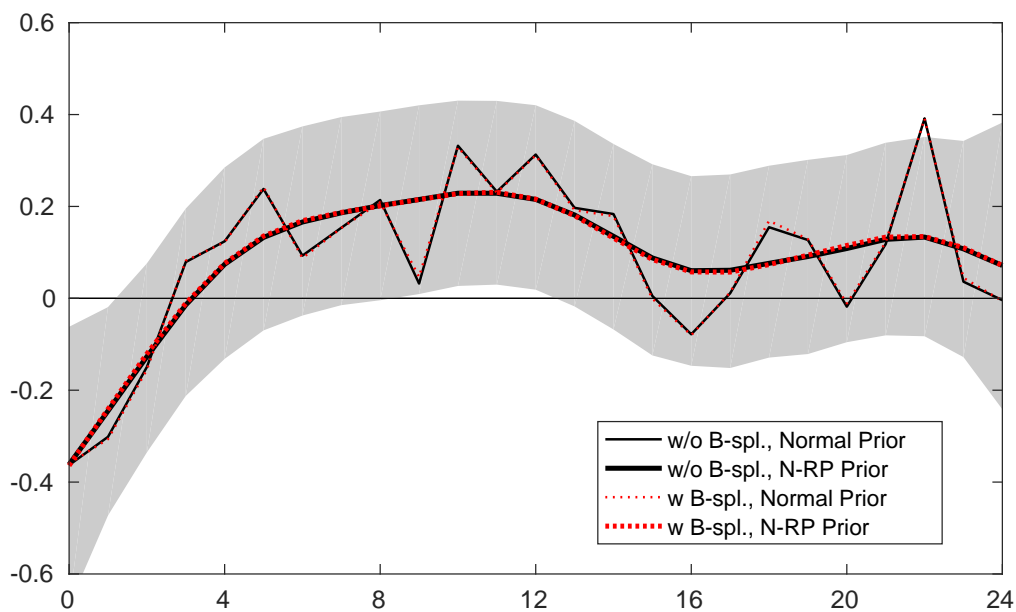
Note: MSE denotes the mean squared error. Speed denotes the computational time in seconds.

Figure 1: B-spline basis



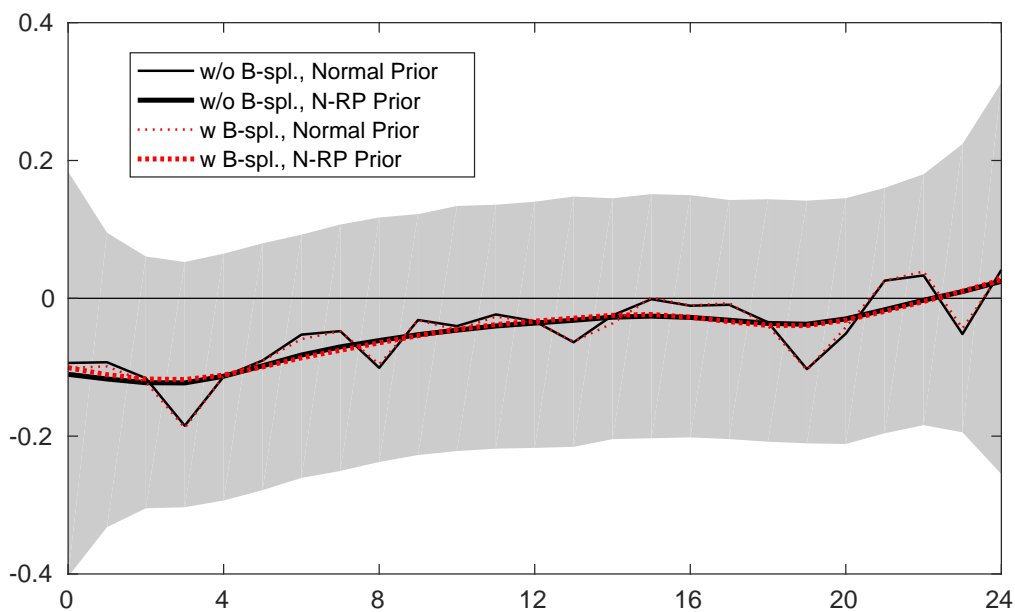
Note: The solid lines show B-spline basis functions used in a functional data analysis (panel (a)) and local projection (panel (b)), respectively. Points are simulated observations for each case. Thick lines highlight the basis functions centered at the sixth knot.

Figure 2: Response of industrial production to monetary policy shocks



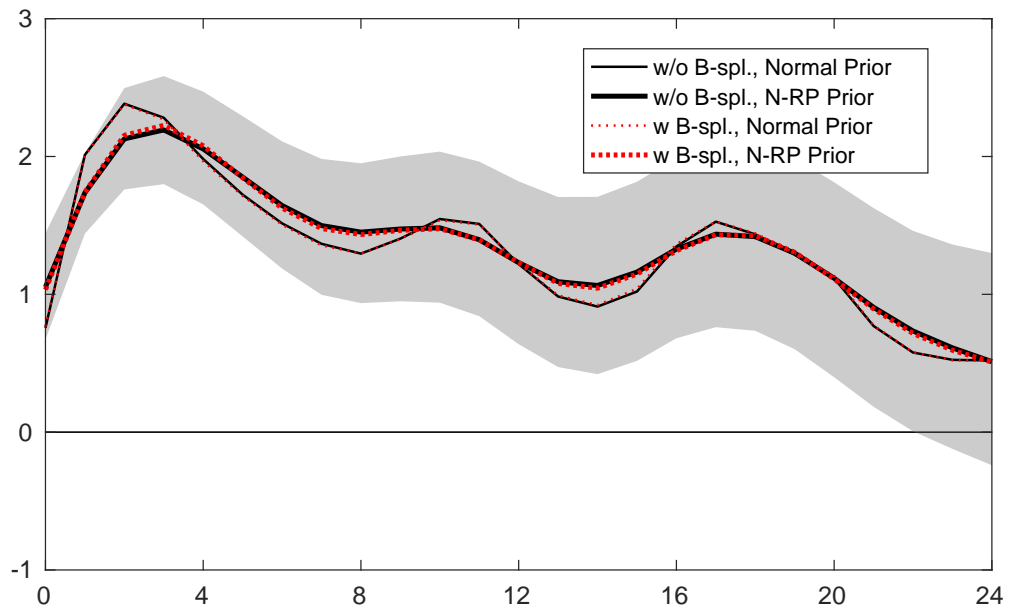
Note: The thin solid line traces the posterior mean for a specification with no B-spline and the normal prior. The thick solid line traces the posterior mean for a specification using no B-spline and the N-RP prior, and the shaded area indicates the corresponding 90% credible set. The thin dotted line traces the posterior mean for a specification with B-splines and the normal prior. The thick dotted line traces the posterior mean for a specification with B-splines and the N-RP prior.

Figure 3: Response of inflation to monetary policy shocks



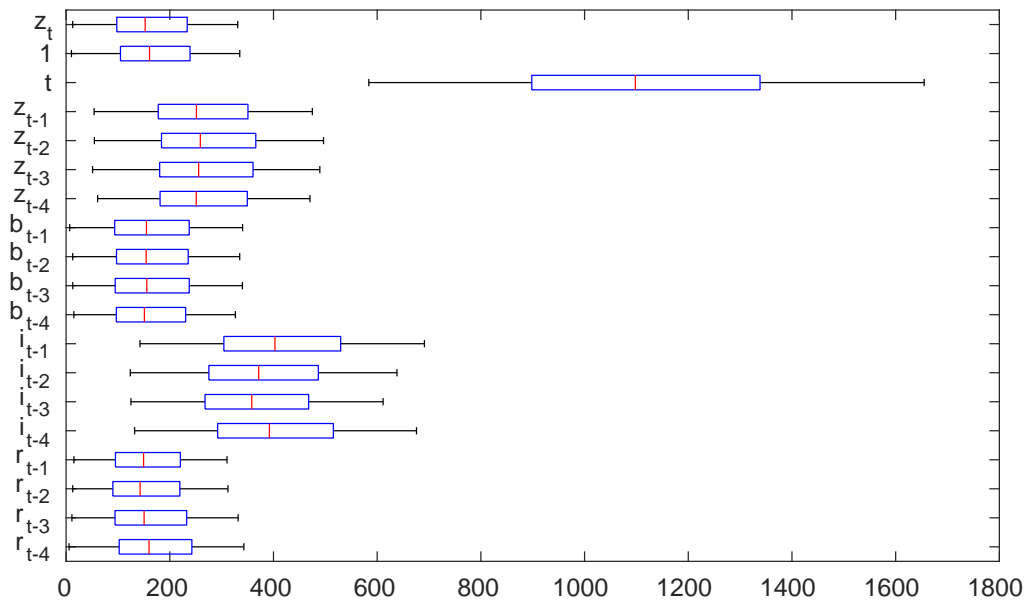
Note: The thin solid line traces the posterior mean for a specification with no B-spline and the normal prior. The thick solid line traces the posterior mean for a specification using no B-spline and the N-RP prior, and the shaded area indicates the corresponding 90% credible set. The thin dotted line traces the posterior mean for a specification with B-splines and the normal prior. The thick dotted line traces the posterior mean for a specification with B-splines and the N-RP prior.

Figure 4: Response of fed funds rate to monetary policy shocks



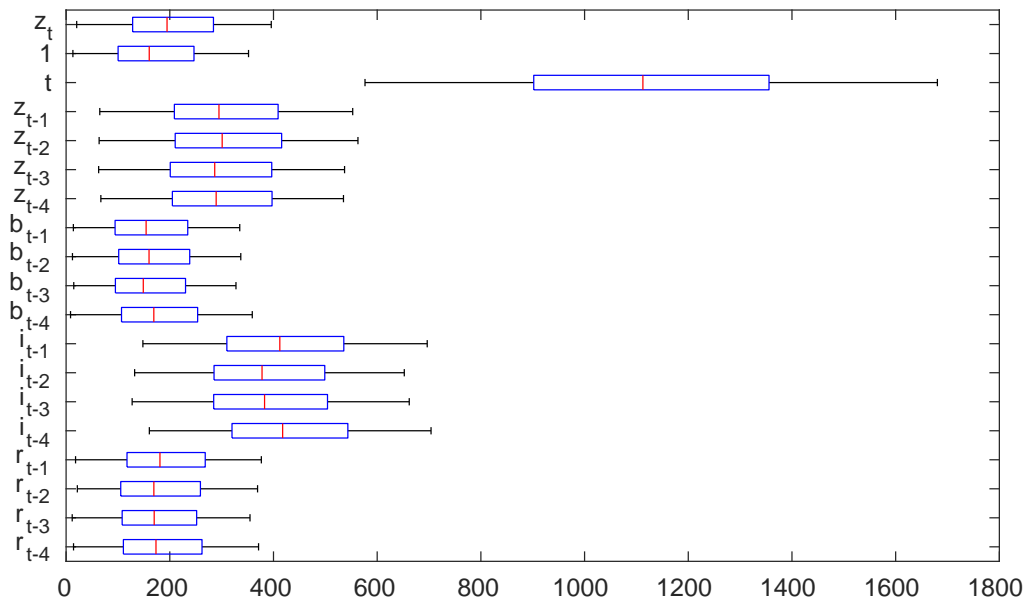
Note: The thin solid line traces the posterior mean for a specification with no B-spline and the normal prior. The thick solid line traces the posterior mean for a specification using no B-spline and the N-RP prior, and the shaded area indicates the corresponding 90% credible set. The thin dotted line traces the posterior mean for a specification with B-splines and the normal prior. The thick dotted line traces the posterior mean for a specification with B-splines and the N-RP prior.

Figure 5: Posterior of smoothing parameter: industrial production



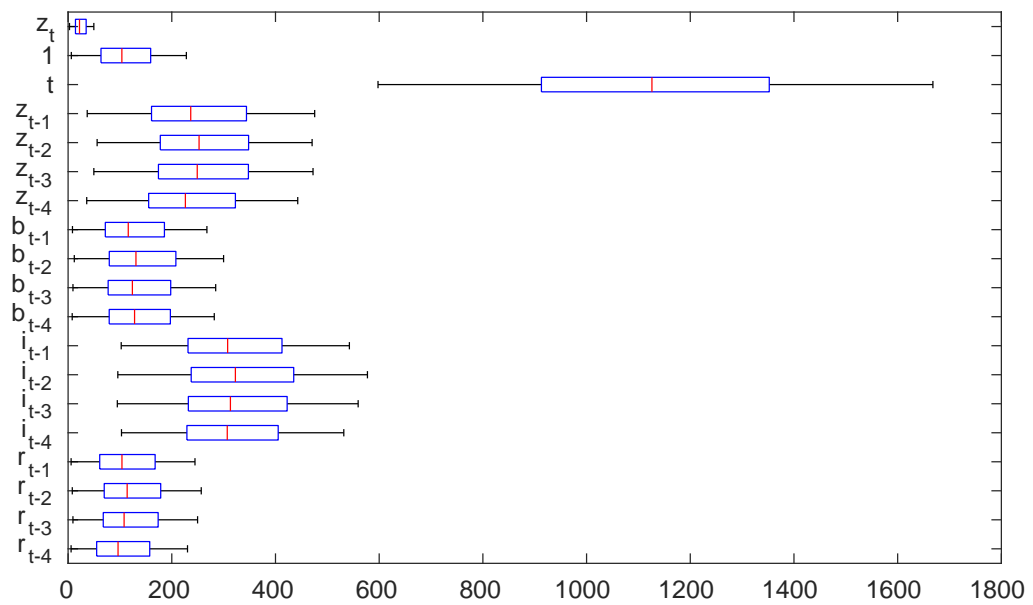
Note: The lines within the boxes denote the posterior median, the edges of the boxes denote the 25th and 75th percentiles of the posterior sample, and the end points of the solid line denote the 5th and 95th percentiles of the posterior sample.

Figure 6: Posterior of smoothing parameter: inflation



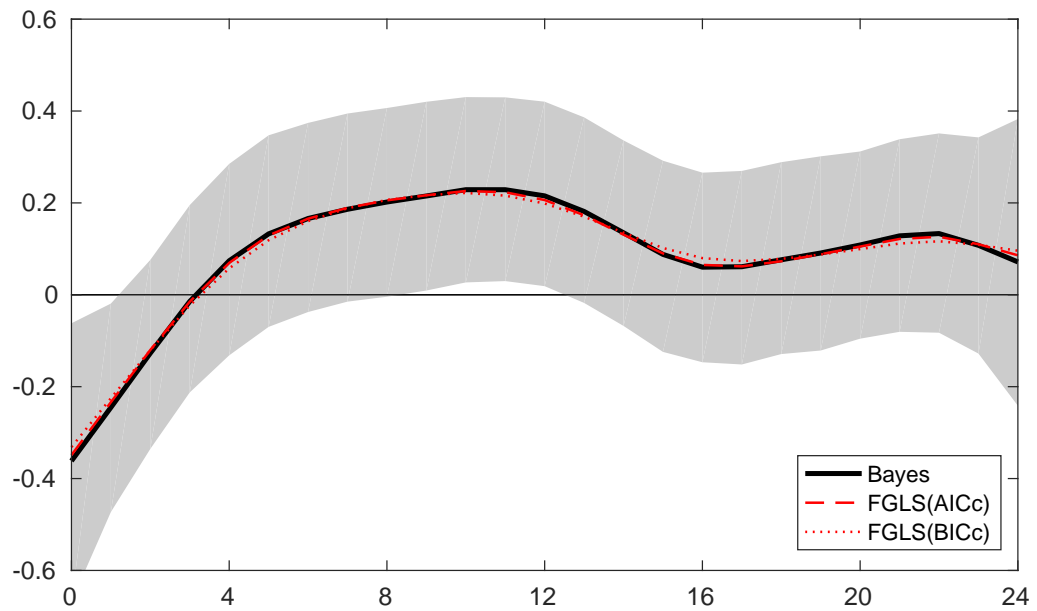
Note: The lines within the boxes denote the posterior median, the edges of the boxes denote the 25th and 75th percentiles of the posterior sample, and the end points of the solid line denote the 5th and 95th percentiles of the posterior sample.

Figure 7: Posterior of smoothing parameter: Fed funds rate



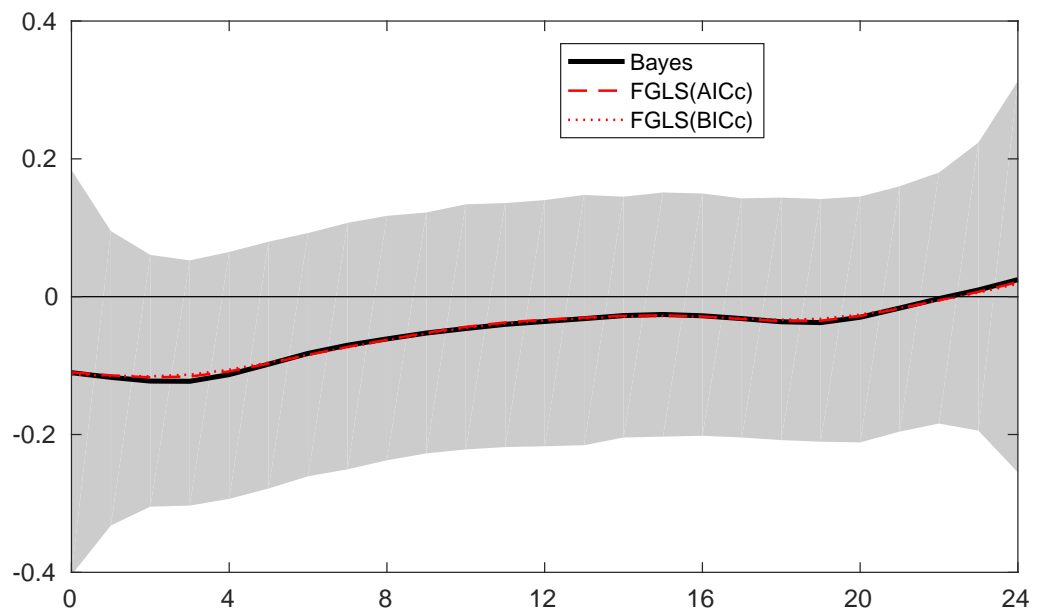
Note: The lines within the boxes denote the posterior median, the edges of the boxes denote the 25th and 75th percentiles of the posterior sample, and the end points of the solid line denote the 5th and 95th percentiles of the posterior sample.

Figure 8: Response of industrial production to monetary policy shocks: frequentist and Bayesian approaches



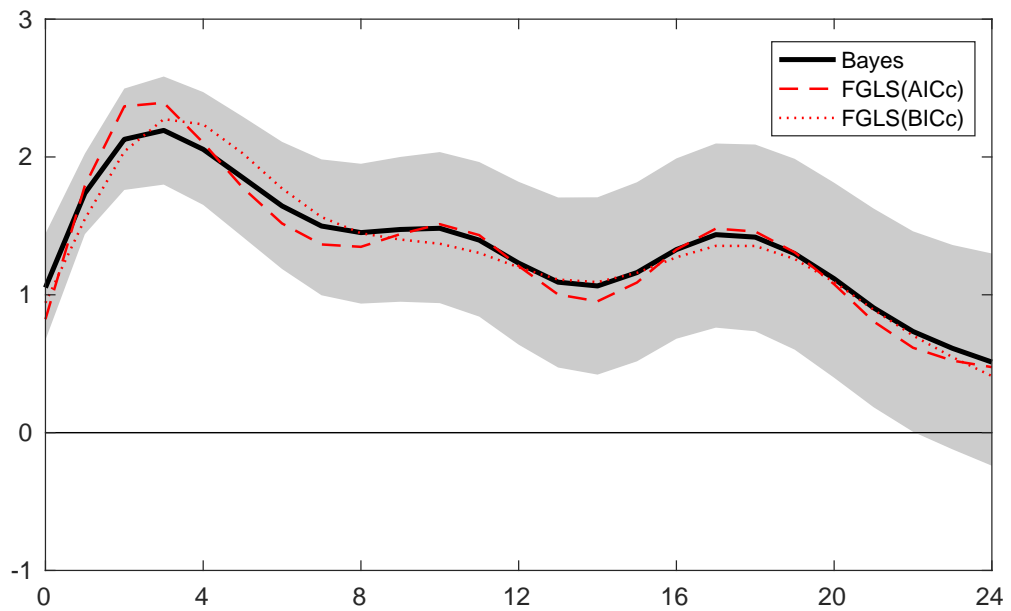
Note: The solid line traces the posterior mean for a Bayesian approach, and the shaded area indicates the corresponding 90% credible set. The dashed line traces an estimate for a frequentist approach with the AICc. The dotted line traces an estimate for a frequentist approach with the BICc.

Figure 9: Response of inflation to monetary policy shocks: frequentist and Bayesian approaches



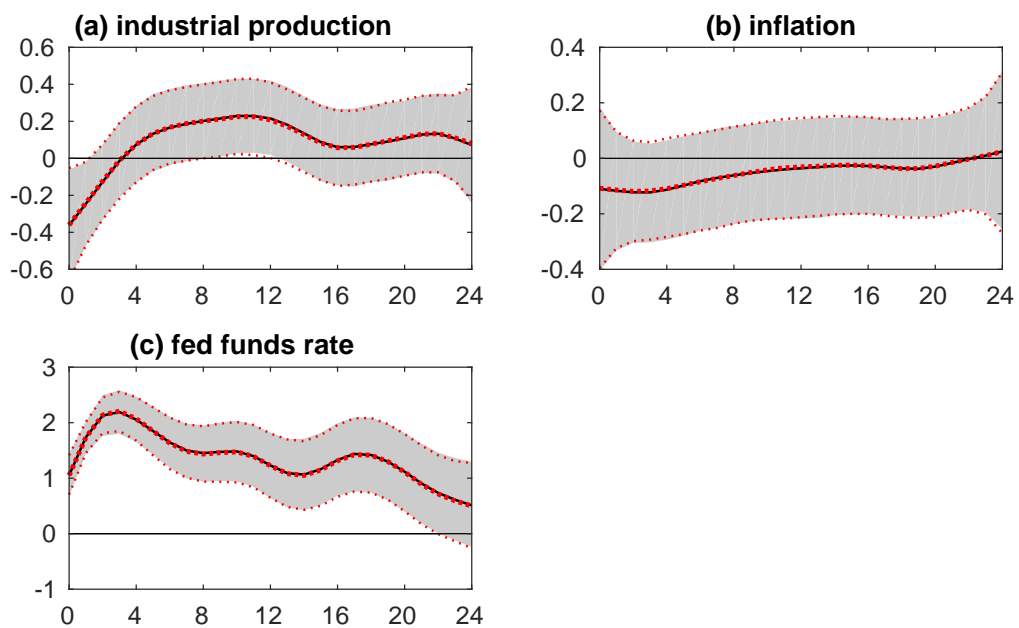
Note: The solid line traces the posterior mean for a Bayesian approach, and the shaded area indicates the corresponding 90% credible set. The dashed line traces an estimate for a frequentist approach with the AICc. The dotted line traces an estimate for a frequentist approach with the BICc.

Figure 10: Response of fed funds rate to monetary policy shocks: frequentist and Bayesian approaches



Note: The solid line traces the posterior mean for a Bayesian approach, and the shaded area indicates the corresponding 90% credible set. The dashed line traces an estimate for a frequentist approach with the AICc. The dotted line traces an estimate for a frequentist approach with the BICc.

Figure 11: Response to monetary policy shocks: inferred and fixed smoothing parameters



Note: The solid black line traces the posterior mean for a model with inferred smoothing parameters. The bold dotted line traces the posterior mean for a model with fixed smoothing parameters. The shaded area indicates a 90% credible set for a model with inferred smoothing parameters. The thin dotted line indicates 90% credible set for a model with fixed smoothing parameters.

Online Appendix to “Bayesian Inference of Local Projections with Roughness Penalty Priors” (not for publication)

Masahiro Tanaka

July 7, 2019

A.1 Inverse Wishart Prior for Σ

This section compare an inverse Wishart prior with the hierarchical inverse Wishart prior we propose. An inverse Wishart prior is specified by

$$\Sigma \sim \mathcal{IW}(\mathbf{I}_H, \xi + H - 1),$$

where ξ is a prefixed hyperparameter. The corresponding conditional posterior is

$$\Sigma|-\sim \mathcal{IW}\left(\Xi + \tilde{\mathbf{U}}^\top \tilde{\mathbf{U}}, H + \xi + T\right).$$

This prior is more popular and simpler than the HIW prior. A simulation environment is the same with the linear case in Section 3 in the main paper. The simulation result is summarized in Table A.1. Though we considered $\xi = 0, 1, 2$, the choice of ξ had almost no effect on the result. Compared to the HIW prior, the inference using the inverse Wishart prior tended to obtain a shorter length, larger MSE and less coverage. Based on the simulation result, we prefer the HIW prior to the inverse Wishart prior.

A.2 Sensitivity Check

We investigated the sensitivity of the inference to the choice of hyperparameters. A simulation setting is adapted from the linear case in Section 3 of the main paper. We considered $\nu = 0.1, 0.01, 0.001, 0.0001$ for models with the N-RP prior and no B-spline. Table A.2 shows the results, wherein two items are noteworthy. First, as long as ν is set between 0.1 and 0.0001, an estimation using the N-RP prior is more efficient than one using the normal prior. Second, we see a bias-variance trade-off: as ν increases (i.e., shrinkage toward 0), an estimator becomes more efficient but less robust. Table A.3 reports the results for $\eta = 1, 0.5, 0.1, 0.01$. We can see that as long as it is chosen within this range, η does not significantly affect the performance. Even when η changes, the A-RP prior cannot beat the N-RP prior. Table A.4 includes the results for $\nu = 0.1, 0.01, 0.001, 0.0001$. There is almost no difference between the results for the alternative specifications, which implies that $\nu = 0.01$

is sufficiently small for the synthetic data. The results for $r = 1, 2, 3, 4$ are shown in Table A.5. While this experiment indicates that $r = 1$ was the best choice, the approach using the N-RP prior consistently outperformed that using the normal prior.

We also conducted a series of sensitivity checks for the real data application in Section 5 of the main paper using the same alternative hyperparameter values above. Figures A.1 to A.4 depict the results for ν , η , v , and r , respectively. We see that choice of the hyperparameters did not affect the shape of the impulse response functions.

Table A.1: Results of the Monte Carlo simulation: inverse Wishart prior for Σ

T	Prior	ξ	MSE	Length	Coverage
50	HIW	–	0.131	0.432	0.994
	IW	0	0.227	0.299	0.851
		1	0.228	0.297	0.849
		2	0.229	0.296	0.842
100	HIW	–	0.067	0.309	0.994
	IW	0	0.090	0.217	0.906
		1	0.090	0.216	0.905
		2	0.090	0.215	0.904

Note: MSE denotes the mean squared error. Coverage denotes the arithmetic mean of the probability that the true value is within a 90% credible interval. Length denotes the length of the 90% credible interval.

Table A.2: Results of the Monte Carlo simulation: sensitivity to the choice of ν

T	Prior	ν	MSE	Length	Coverage
50	Normal	–	0.542	0.976	0.997
		0.1	0.180	0.526	0.995
	N-RP	0.01	0.131	0.432	0.994
		0.001	0.099	0.367	0.993
		0.0001	0.079	0.324	0.993
100	Normal	–	0.243	0.599	0.995
		0.1	0.090	0.378	0.995
	N-RP	0.01	0.067	0.309	0.994
		0.001	0.053	0.261	0.990
		0.0001	0.043	0.228	0.989

Note: MSE denotes the mean squared error. Coverage denotes the arithmetic mean of the probability that the true value is within a 90% credible interval. Length denotes the length of the 90% credible interval.

Table A.3: Results of the Monte Carlo simulation: sensitivity to the choice of η

T	Prior	η	MSE	Length	Coverage
50	Normal	–	0.542	0.976	0.997
	N-RP	–	0.131	0.432	0.994
	A-RP	1.0	0.143	0.454	0.994
		0.5	0.150	0.468	0.994
		0.1	0.163	0.494	0.995
		0.01	0.157	0.481	0.994
	Normal	–	0.243	0.599	0.995
	N-RP	–	0.067	0.309	0.994
100	1.0	0.072	0.323	0.994	
	A-RP	0.5	0.074	0.331	0.995
		0.1	0.078	0.344	0.995
		0.01	0.074	0.332	0.994

Note: MSE denotes the mean squared error. Coverage denotes the arithmetic mean of the probability that the true value is within a 90% credible interval. Length denotes the length of the 90% credible interval.

Table A.4: Results of the Monte Carlo simulation: sensitivity to the choice of ν

T	Prior	ν	MSE	Length	Coverage
50	Normal	–	0.542	0.976	0.997
		0.1	0.130	0.438	0.995
	N-RP	0.01	0.131	0.432	0.994
		0.001	0.131	0.432	0.994
		0.0001	0.131	0.432	0.994
100	Normal	–	0.243	0.599	0.995
		0.1	0.067	0.314	0.995
	N-RP	0.01	0.067	0.309	0.994
		0.001	0.067	0.309	0.994
		0.0001	0.067	0.309	0.993

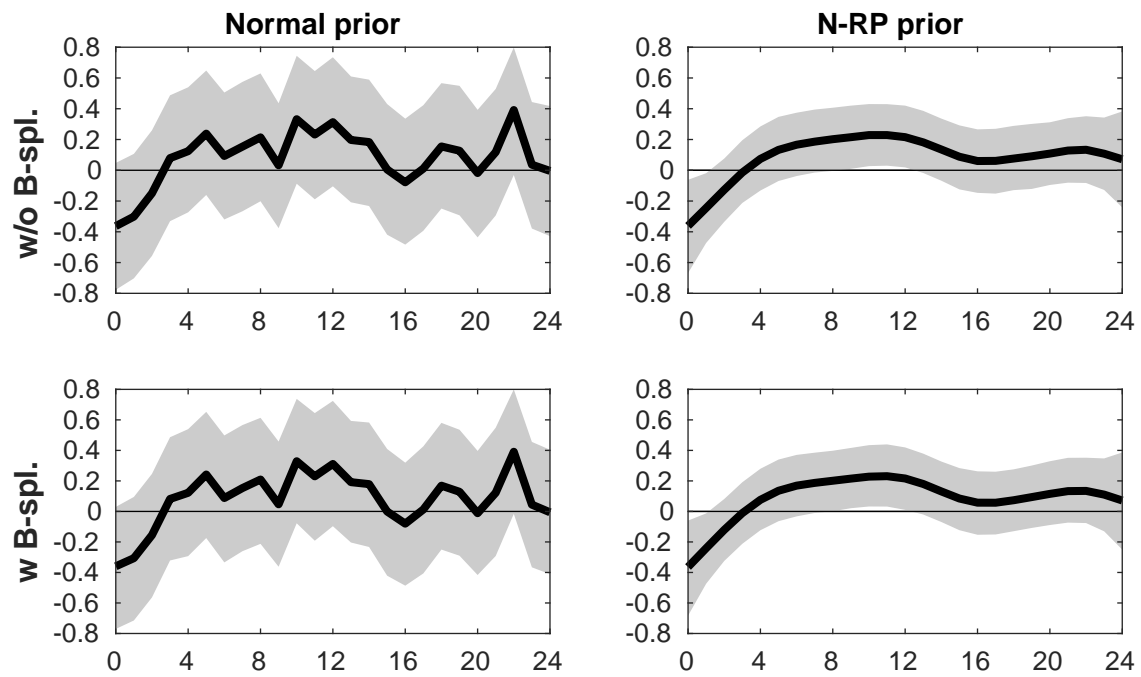
Note: MSE denotes the mean squared error. Coverage denotes the arithmetic mean of the probability that the true value is within a 90% credible interval. Length denotes the length of the 90% credible interval.

Table A.5: Results of the Monte Carlo simulation: sensitivity to choice of r

T	Prior	r	MSE	Length	Coverage
50	Normal	–	0.542	0.976	0.997
		N-RP	1	0.077	0.381
	2		0.131	0.432	0.994
	3		0.169	0.471	0.993
	4	0.197	0.503	0.991	
100	Normal	–	0.243	0.599	0.995
		N-RP	1	0.046	0.287
	2		0.067	0.309	0.994
	3		0.081	0.328	0.990
	4	0.090	0.344	0.990	

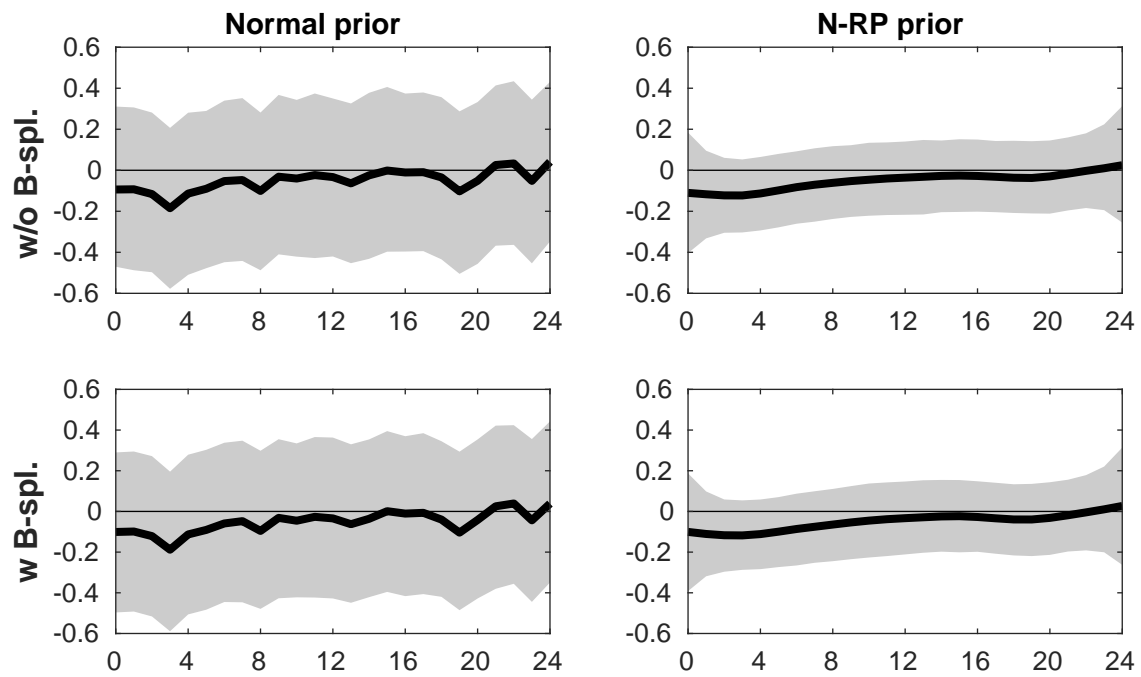
Note: MSE denotes the mean squared error. Coverage denotes the arithmetic mean of the probability that the true value is within a 90% credible interval. Length denotes the length of the 90% credible interval.

Figure A.1: Response of industrial production to monetary policy shocks



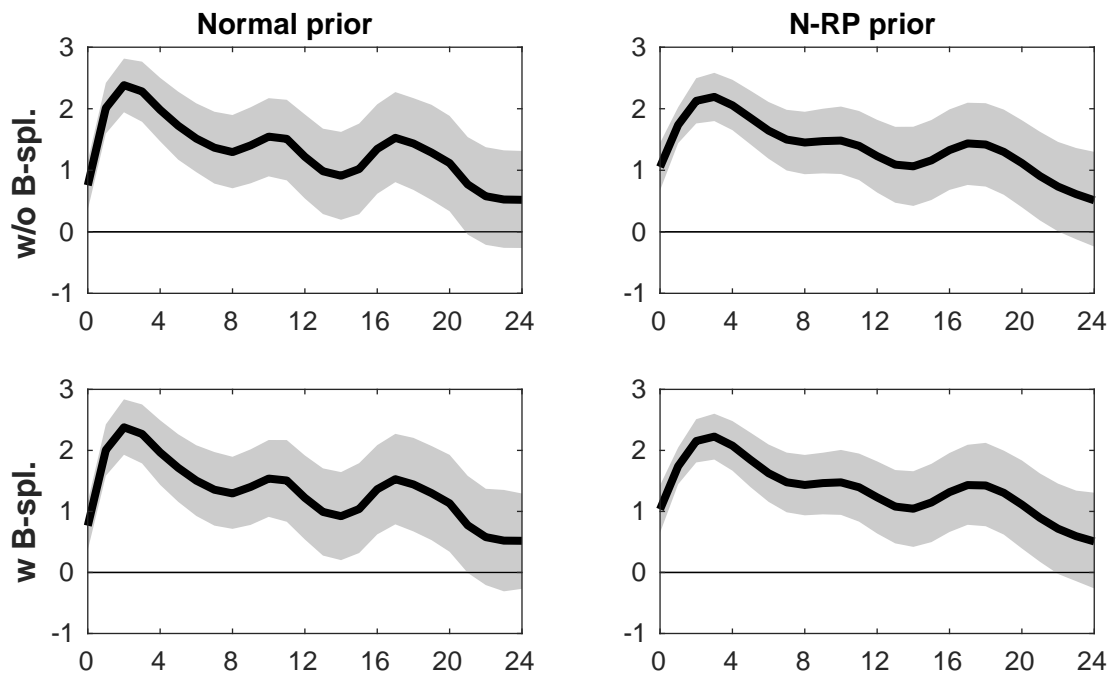
Note: The thick lines trace the posterior mean. The shaded area indicates the 90% credible set.

Figure A.2: Response of inflation to monetary policy shocks



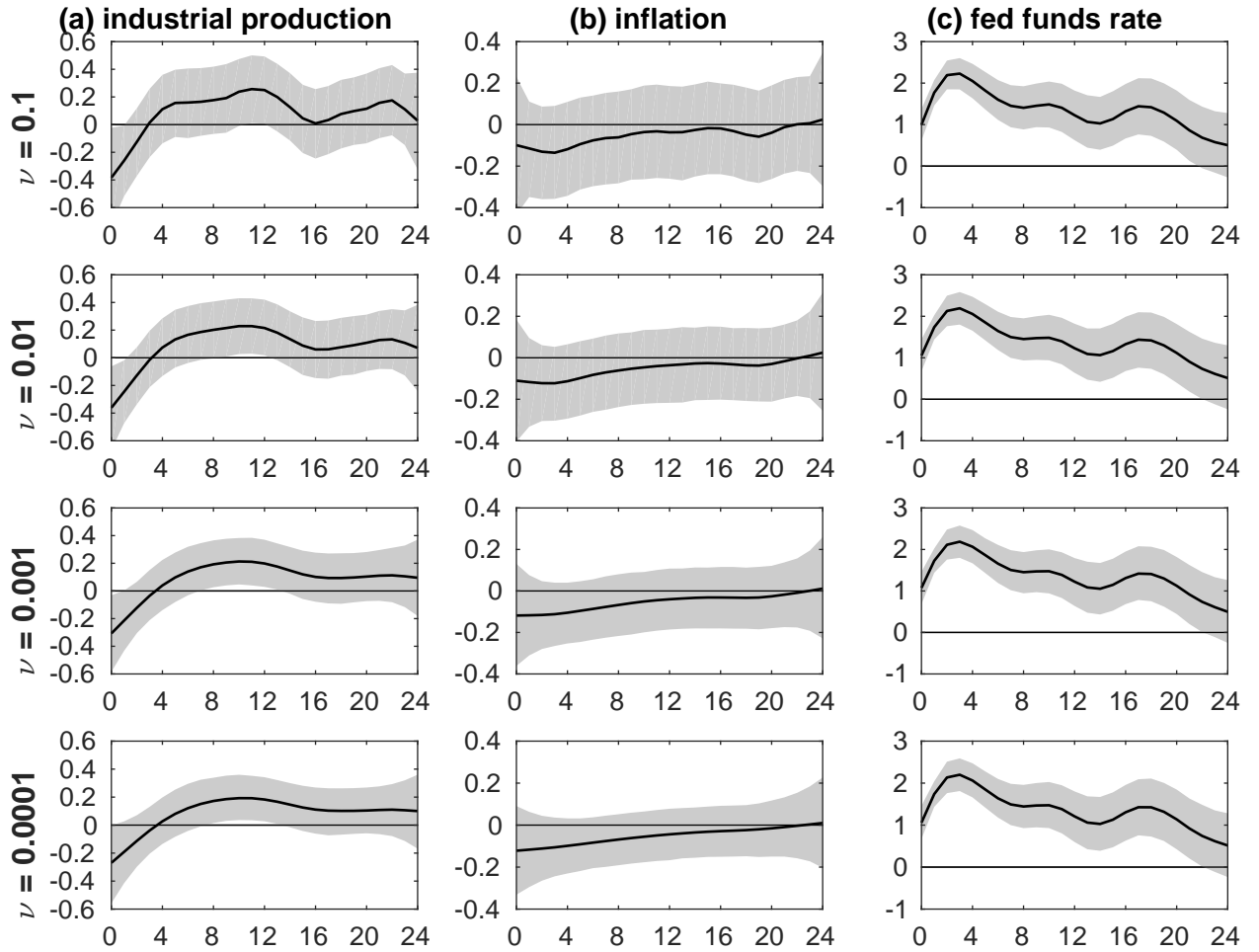
Note: The thick lines trace the posterior mean. The shaded area indicates the 90% credible set.

Figure A.3: Response of the Fed funds rate to monetary policy shocks



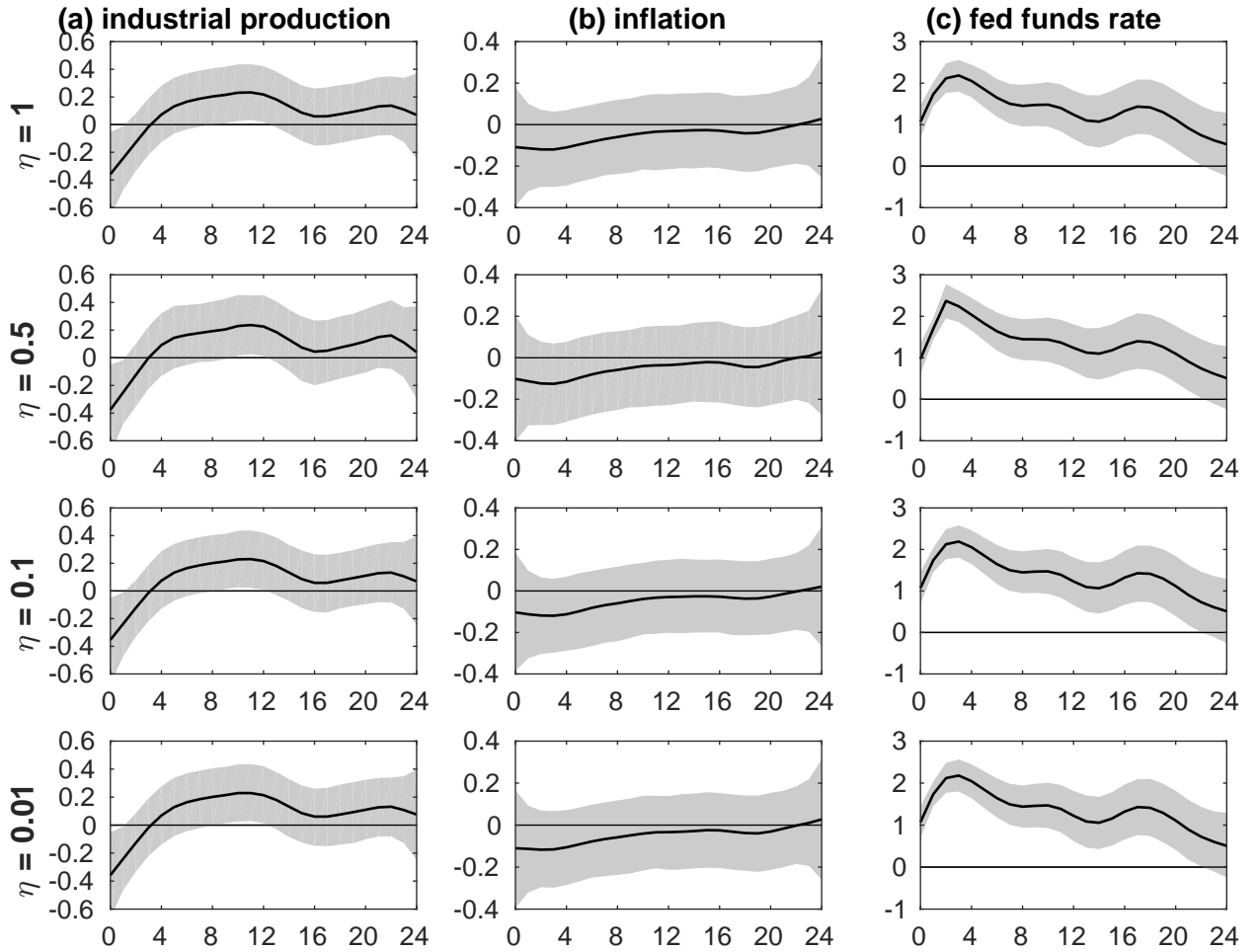
Note: Thick lines trace the posterior mean. The shaded area indicates the 90% credible set.

Figure A.4: Response to monetary policy shocks: sensitivity to ν



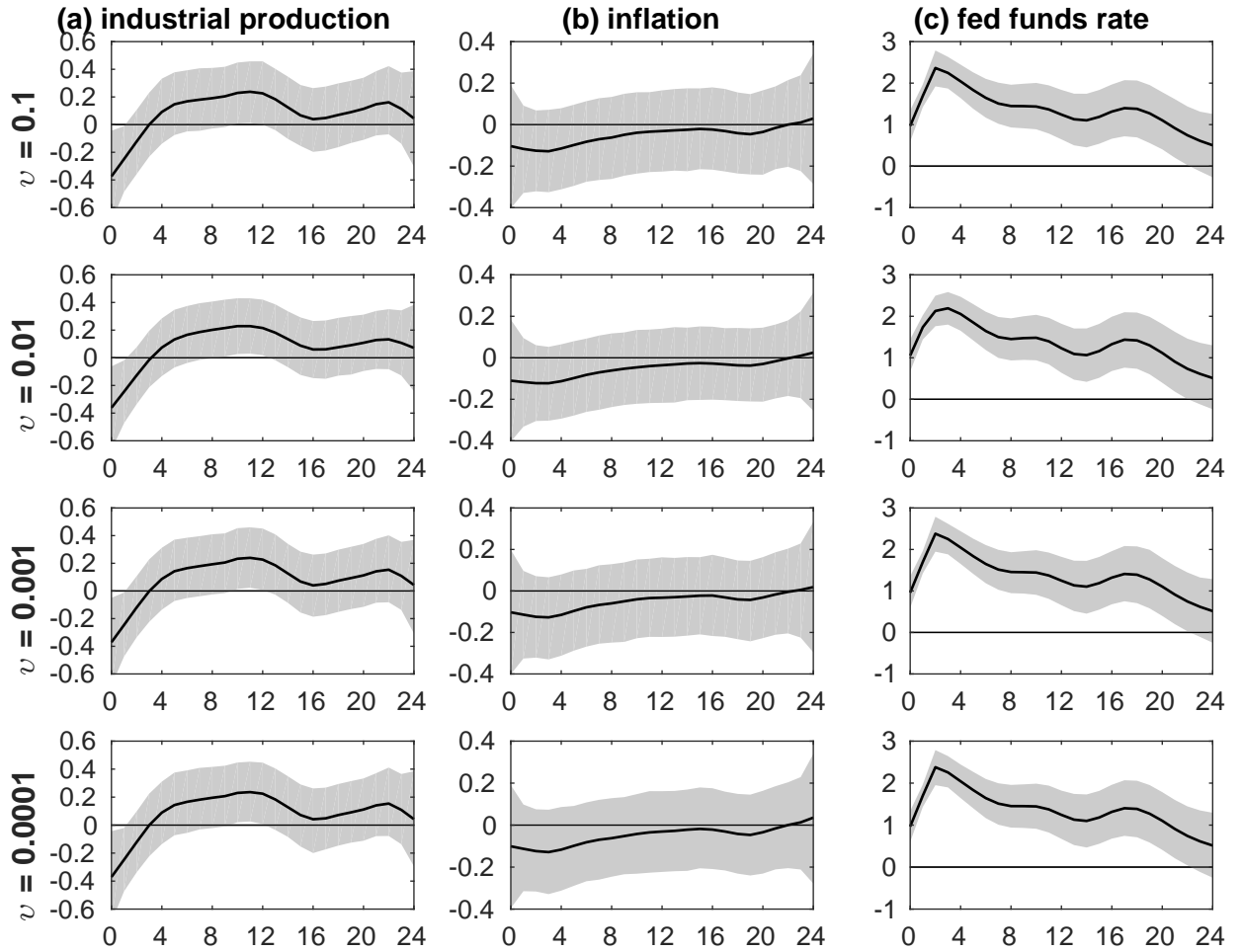
Note: Thick lines trace the posterior mean. Shaded area indicates 90% credible set.

Figure A.5: Response to monetary policy shocks: sensitivity to η



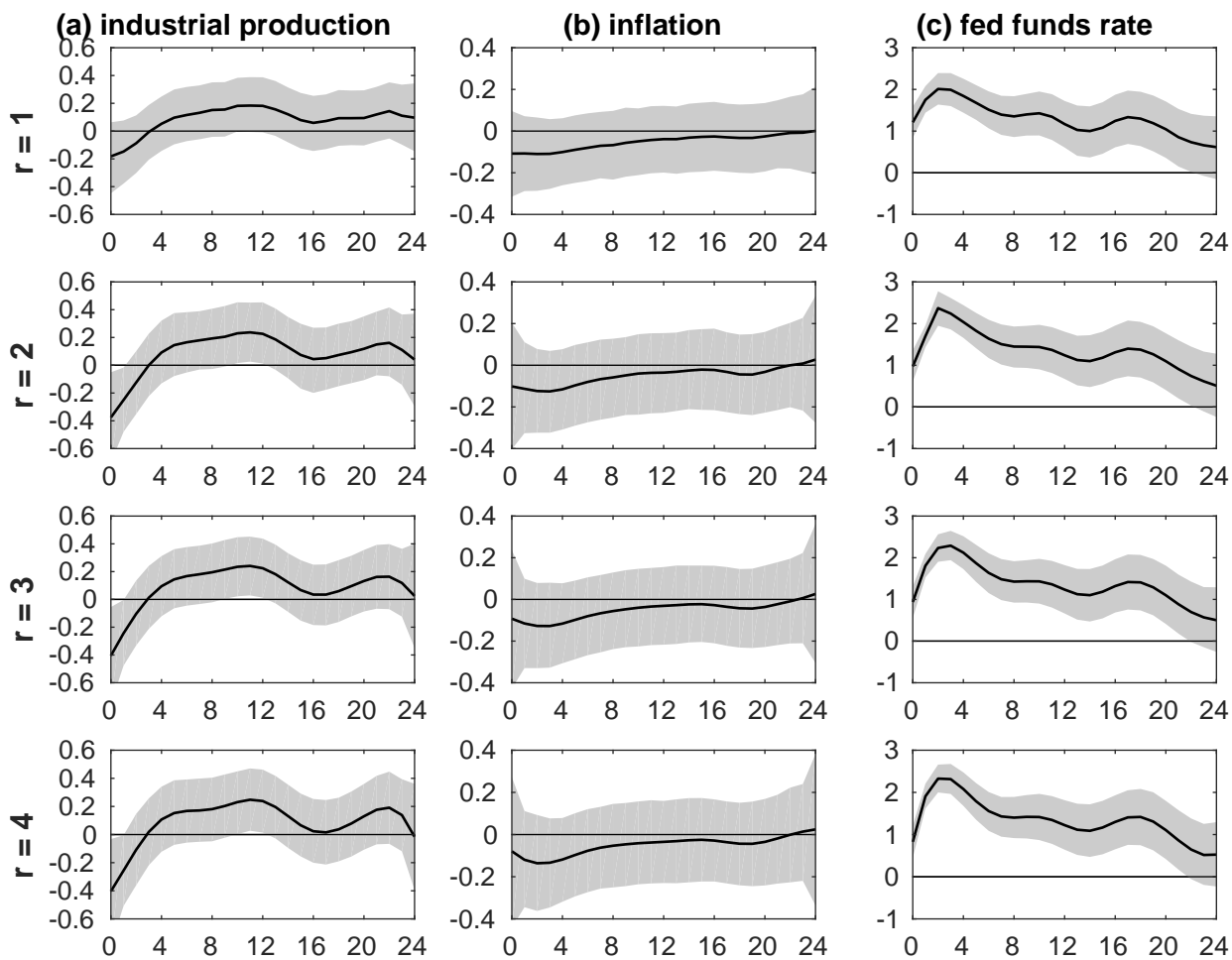
Note: Thick lines trace the posterior mean. Shaded area indicates 90% credible set.

Figure A.6: Response to monetary policy shocks: sensitivity to v



Note: Thick lines trace the posterior mean. Shaded area indicates 90% credible set.

Figure A.7: Response to monetary policy shocks: sensitivity to r



Note: Thick lines trace the posterior mean. Shaded area indicates 90% credible set.